



TECHNICAL REPORT

“Assessment of six batches of tungsten bricks (intended for the target of the ESS) according to a technical selection protocol agreed with ESS-Bilbao. Stage 1 results”

Document Code: MT / 120033 / 15

/ R 01

CONFIDENTIAL

Donostia- San Sebastián

ELABORATED
Nerea Ordás Mur, Carmen García-Rosales, Antonio Martín Meizoso, Javier Aldazabal, Amaia Gómez, José Luis Pedrejón, Javier Gil sevillano
Date: 15/01/2016



CONFIDENTIAL

Section: OBJECTIVE OF THIS STUDY

Contents

1	OBJECTIVE OF THIS STUDY	5
2	RESULTS.....	7
2.1	CHEMICAL COMPOSITION	7
2.2	MASS DENSITY	9
2.3	YOUNG ELASTIC MODULUS (SHORT-TRANSVERSE DIRECTION)	11
2.4	VICKERS HARDNESS (AS-RECEIVED ROLLING SURFACE, 1 kg)	13
2.5	RESIDUAL STRESSES (AS-RECEIVED ROLLING SURFACE).....	15
2.6	TENSILE STRENGTH AT ROOM TEMPERATURE, L AND T DIRECTIONS.....	18
2.7	FRACTOGRAPHY	21
3	SUMMARY AND FINAL COMMENTS	43



CONFIDENTIAL

Section: OBJECTIVE OF THIS STUDY

1 OBJECTIVE OF THIS STUDY

Ceit-IK4 has received from ESS-Bilbao samples from 6 different suppliers of pure tungsten (2 bricks per supplier) for their characterization in order to select the definitive supplier of the ESS target material. The list of tests and their conditions to be performed were suggested by Ceit-IK4 on the basis of a preliminary study (Ceit IK4 technical report MT/120029/15/R01), “A testing protocol for selection of tungsten bricks for the target of the European Neutron Spallation Source, ESS”).

The bricks were identified by a numeral (from 1 to 6, two specimens from each batch, ref. 1 or 2). Ceit-IK4 was blind towards the identity of brick suppliers.

The bricks were visually inspected (fig.1) and the following list of properties were measured from samples extracted by EDM (electro discharge machining) from the bricks (intact bricks were employed for measuring the elastic modulus by ultrasounds):

- Chemical composition (C, S, O, N)
- Mass density
- Young elastic modulus in short-transverse direction (full thickness)
- HV (1kg) Vickers hardness (on the rolling plane, as-received surface)
- Residual stresses in the as-received surface
- Tensile strength measured at RT in 3P bending¹ with the tensile failure nucleating from the as-received (intact) surface of the bricks (rolling plane)
- Fracture surface characteristics

The results of this battery of tests will be used for filtering three potentially valid suppliers. Any gross departure from the expected properties of rolled pure tungsten will discard a supplier (for instance, a minimal tensile strength of 600 MPa was specified by ESS-Bilbao as a necessary condition for acceptance of a batch of bricks). A deeper study of the three candidates having passed the filter is to be done for the final selection.

¹ In a first instance (Appendix 1), the tensile strength was to be measured by tensile tests. After machining the tensile samples, difficulties encountered after performing several trials of the tests (early brittle fractures at the shoulders of the samples associated to gripping and loading misalignment problems) lead to performing 3P bending tests using the same geometry employed for tungsten by other laboratories in recent papers).



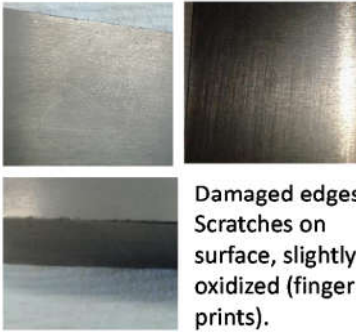



<p>1</p>  <p>Grey spots (oxide) on surface</p>	<p>2</p>  <p>Thin continuous (oxide) layer on surface</p>	<p>3</p>  <p>Damaged edges. Scratches on surface, slightly oxidized (finger prints).</p>
<p>4</p>  <p>Bright smooth surface, free from oxides</p>	<p>5</p>  <p>Brightest, smoothest surface, probably polished. Free from oxides</p>	<p>6</p>  <p>Rough surface, free from oxides. Bricks slightly shorter??</p>

Figure 1. Visual aspect of the as-received bricks.

2 RESULTS

2.1 CHEMICAL COMPOSITION

Carbon and sulphur concentration were analysed by the induction furnace method (ASTM E 1941-10, *Standard Test Method for Determination of Carbon in Refractory and Reactive Metals and Their Alloys by Combustion Analysis*) by means of a Leco CS200 equipment. A Leco sample for C and S (composition and traceability supplied by Leco) was used for calibration.

The concentration of nitrogen and oxygen was measured by the inert gas fusion method (ASTM E1569-09, *Standard Test Method for Determination of Oxygen in Tantalum Powder by Inert Gas Fusion Technique*). The equipment used for measurement was a Leco TC-400. A Leco sample (composition and traceability supplied by Leco) was used for calibration.

A minimum of 3 independent measurements were performed for each element and sample, as recommended for the method and equipment used.

The results are detailed in Table 1.

TABLE 1. Chemical composition of W bricks

Content (ppm)		supplier					
	meas.	1	2	3	4	5	6
C	1	8.0	6.8	4,3	5,8	3.2	5,6
	2	9.2	8,3	1,7	4.5	13.4	8,4
	3	8.7	6,5	4,8	8.2	5.8	6,9
	Av	8.6	7.2	3.6	6.2	7.5	7.0
	Stdev	0.6	1.0	1.7	1.9	5.3	1.4
S	1	0.9	0	0,2	0,3	0.1	0
	2	0	0,1	0,1	0,2	0.3	0
	3	0	0	0	0,3	0.6	0
	Av	0.3	0.03	0.1	0.3	0.3	0
	Stdev	0.4	0.1	0.1	0.1	0.3	0
O	1	10.5	17.3	4.4	9.1	17.2	5.5
	2	7.0	11.5	16.7	9.5	49.7	3.1
	3	3.8	20.9	6.4	13.5	67.6	3.6
	4	2.6	7.1			27.6	
	5		11.9			28.1	
	6					72.5	
	7					47.8	
	Av	6	13.7	9.2	10.7	44.4	4.3
	Stdev	3.5	5.4	6.6	2.4	21.0	1.3
N	1	4.0	0	1	0.1	0	0.5
	2	0.3	0.1	4.4	0	0.1	0.6
	3	1.3	0.4	0	0	0.2	0.2
	4	0	0			0.2	
	5		6.4			0.1	
	Av	1.4	1.4	1.5	0	0.1	0.4
	Stdev	1.8	2.9	2.5	0.1	0.1	0.2

All samples show <15 ppm of any impurity but for sample 5 which has on average >30 ppm O (above the considered threshold for O content, 30 ppm). Available results in the literature, however, estimate that a much higher oxygen concentration is required for having an impact on the mechanical properties of pure tungsten.

2.2 MASS DENSITY

Mass density has been measured at room temperature both by the “geometric” method (volume measured from the external geometry of the bricks) and by the Archimedes “inmersion” water displacement method according to ASTM B311-13, *Standard Test Method for Density of Powder Metallurgy (PM) Materials Containing Less than Two Percent Porosity*.

Detailed results are given in Table 2.

TABLE 2. MASS DENSITY OF W BRICKS

	code	dimensions (mm)			mass (g)	density (g/cm ³)	Inmer. density (g/cm ³)
		L1	L2	H			
1	A	0,755333	3	0,07102	3,0224	18,78069	18,79537
	RS						
	B	0,76	3	0,07158	3,0868	18,91394	19,1125
	Av	0,758	3,000	0,071	3,055	18,847	18,954
	Stdev	0,003	0,000	0,000	0,046	0,094	0,224
2	A	3	3	0,88466	152,3394	19,13345	19,23309
	RS	2,468	3	0,99778	141,7361	19,18577	19,21672
	B	2,473	3	0,88648	125,9123	19,14493	19,17444
	Av	2,647	3	0,923	139,996	19,155	19,208
	Stdev	0,306	0,000	0,065	13,299	0,027	0,030
3	A	3	3	0,88482	140,3476	17,62412	17,72584
	RS	2,472	3	0,99786	130,421	17,62415	17,68309
	B	2,47	3	0,88182	114,7395	17,55961	17,66886
	Av	2,647	3,000	0,922	128,503	17,603	17,693
	Stdev	0,305	0,000	0,066	12,911	0,037	0,030
4	A	2,472	3	0,9969	142,3324	19,25229	19,23531
	RS	3	3	0,88462	152,7876	19,19061	19,19511
	B	2,468	3	0,88428	125,4567	19,16186	19,17994
	Av	2,647	3,000	0,922	140,192	19,202	19,203
	Stdev	0,306	0,000	0,065	13,791	0,046	0,029
5	A	3	3	0,88086	151,5286	19,11372	19,23359
	RS	2,49	3	0,9933	141,9596	19,13215	19,22422
	B	2,46	3	0,88144	124,352	19,11629	19,23658
	Av	2,65	3	0,919	139,280	19,121	19,231
	Stdev	0,30348	0	0,065	13,785	0,010	0,006
6	A	2,48	3	0,99818	142,5536	19,19537	19,16398
	RS	3	3	0,88458	152,4087	19,14389	19,1864
	B	2,464	3	0,88598	124,9673	19,08141	19,09576
	Av	2,648	3,000	0,923	139,977	19,140	19,149
	Stdev	0,305	0,000	0,065	13,901	0,057	0,047

2.3 YOUNG ELASTIC MODULUS (SHORT-TRANSVERSE DIRECTION)

The Young elastic modulus of the bricks has been measured at room temperature according to ASTM E494-10, *Standard Practice for Measuring Ultrasonic Velocity in Materials*. The velocity of sound was measured in the through-the-thickness direction (normal to the rolling plane) by means of a GE USM/DMS Go apparatus.

A summary of the average results is given below (Table 3). The results are given in detail in Table 4. The associated error to each value is calculated on account of the dispersion and of the instrumental error (according to propagation of errors theory).

TABLE 3. Young modulus of W bricks, average values, RT

Sample	E / GPa	Error
BWT 1.2	403,9	0,7
BWT 2.2	405,9	0,8
BWT 3.2	364,9	0,7
BWT 4.2	408,1	0,8
BWT 5.2	406,4	0,8
BWT 6.2	391,4	0,7

Pure tungsten Young moduli at room temperature, as quoted in the bibliography, are in the range 390-490 GPa. Tungsten is elastically isotropous.

TABLE 4. YOUNG MODULUS OF W BRICKS AT ROOM TEMPERATURE

Muestra	Altura/mm	Anchura/mm	Grosor/mm	Vel_min_9,99/ms ⁻²	Vel_max_9,99/ms ⁻²	Velocidad_esp/ms ⁻²	masa/g
BWT 1.2	80,16	29,97	10	5178	5182	5183	461,50
	80,16	29,97	10	5188	5192	5193	461,50
	80,17	29,96	9,99	5168	5172	5173	461,50
Media	80,1633333	29,9666667	9,99666667			5183	461,50
Error	0,01	0,01	0,01			1	0,01
Volumen/mm³	24014	Error	35				
Densidad/kg m³	19218	Error	28				
E / GPa	403,88	Error	0,75				
BWT 2.2	80,07	30	9,99	5198	5203	5203	459,89
	80,11	30	9,99	5202	5206	5206	459,89
	80,07	29,99	10	5202	5206	5206	459,89
Media	80,0833333	29,9966667	9,99333333			5205	459,89
Error	0,02	0,01	0,01			1	0,01
Volumen/mm³	24006	Error	38				
Densidad/kg m³	19157	Error	30				
E / GPa	405,91	Error	0,80				
BWT 3.2	80,05	30	9,99	5051	5057	5056	438,01
	80,06	30	9,98	5038	5043	5043	438,01
	80,06	30	9,98	5058	5062	5062	438,01
Media	80,0566667	30	9,98333333			5054	438,01
Error	0,01	0,01	0,01			1	0,01
Volumen/mm³	23977	Error	35				
Densidad/kg m³	18268	Error	27				
E / GPa	364,93	Error	0,68				
BWT 4.2	80,02	30	9,99	5205	5210	5204	460,90
	80,01	30	9,99	5219	5223	5218	460,91
	80	29,98	9,97	5202	5206	5201	460,91
Media	80,01	29,9933333	9,98333333			5207	460,91
Error	0,01	0,01	0,01			1	0,01
Volumen/mm³	23958	Error	35				
Densidad/kg m³	19238	Error	28				
E / GPa	408,06	Error	0,75				
BWT 5.2	80,06	29,95	9,96	5204	5208	5203	459,25
	80,05	29,96	9,96	5197	5202	5196	459,25
	80,05	29,96	9,97	5201	5205	5200	459,25
Media	80,0533333	29,9566667	9,96333333			5199	459,25
Error	0,01	0,01	0,01			1	0,01
Volumen/mm³	23893	Error	35				
Densidad/kg m³	19221	Error	28				
E / GPa	406,43	Error	0,75				
BWT 6.2	80,09	29,97	9,98	5096	5101	5101	461,50
	80,09	29,98	9,99	5093	5099	5098	461,50
	80,09	29,97	9,98	5090	5094	5094	461,50
Media	80,09	29,9733333	9,98333333			5098	461,50
Error	0,01	0,01	0,01			1	0,01
Volumen/mm³	23966	Error	35				
Densidad/kg m³	19257	Error	28				
E / GPa	391,40	Error	0,73				

2.4 VICKERS HARDNESS (AS-RECEIVED ROLLING SURFACE, 1 kg)

Vickers hardness tests have been performed at room temperature, on the rolling surface of the bricks, using a load of 1 kg according to ASTM E384-11e1, *Standard Test Method for Knoop and Vickers Hardness of Materials*.

The indentations were performed on the rolling surface without any preparation, the surface state was adequate enough for obtaining clear and acceptable imprints under the 1kg load. Each average hardness value is the result of 20 indentations. The measurements were performed with an automatic Vickers hardness tester modelo Q30 A+ de Qness.

The summary of results is given in Table 5.

TABLE 4. VICKERS HARDNESS (1 kg) OF THE W BRICKS

W supplier	HV (1 kg), ROLLING PLANE kg mm⁻² Average ± 95% cl
1	423.7 ± 25.7
2	496.5 ± 9.5
3	355 ± 6
4	496 ± 6.0
5	412 ± 16
6	470 ± 5.0

Some examples of detailed measurements are given in fig. 2, below.

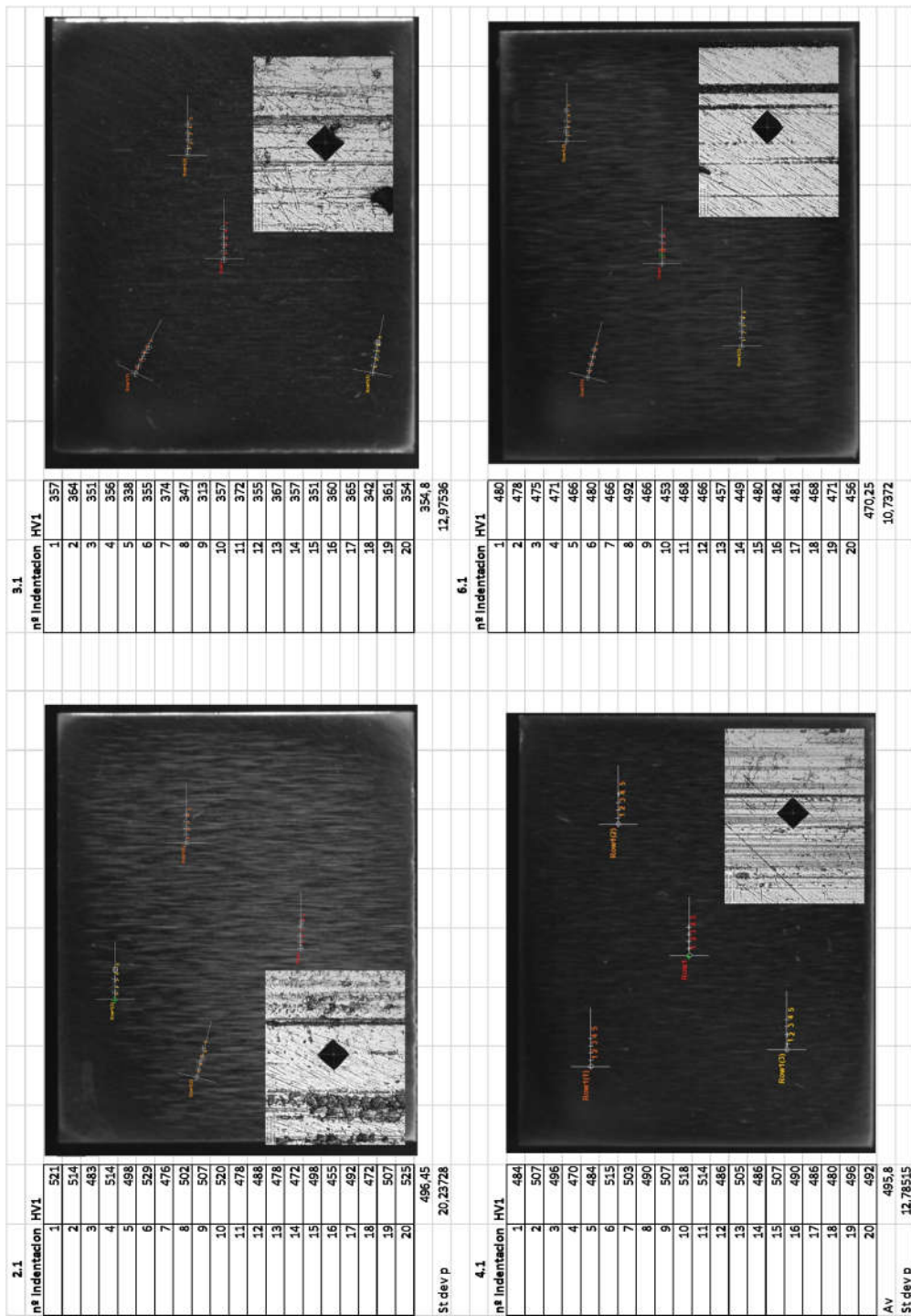


Figure 2. Detailed results, location and example of HV imprint, samples 2.1, 3.1, 4.1, 6.1.

2.5 RESIDUAL STRESSES (AS-RECEIVED ROLLING SURFACE)

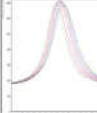
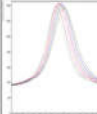
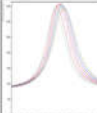
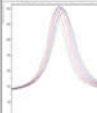
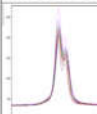
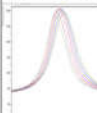
The stress state at the surface of the bricks (rolling plane, as received surface) has been measured by X-ray diffraction using the $\sin 2\psi$ method, according to ASTM E2860-12, *Standard Test Method for Residual Stress Measurement by X-Ray Diffraction for Bearing Steels* (applied to W).

The measurements have been performed in a Philips X'Pert MRD apparatus.

Measurement performed on lattice plane (321) using Cu $K\alpha$ radiation ($2\theta = 131^\circ$). All samples display biaxial compressive stress state.

TABLE 6.

RESIDUAL STRESSES AT THE AS-RECEIVED SURFACE OF THE W BRICKS

Supplier	Residual stress (MPa)				Elastic constants		Peak size	Comments
	σ_L	StdDev	σ_T	StdDev	E (Gpa)*	ν *		
1	-1276	9	-1074	13	406	0.28		Broad diffraction peaks --> plastic deformation (micro-stresses)
2	-789	11	-1088	9				Broad diffraction peaks --> plastic deformation (micro-stresses)
3	-956	20	-1166	8				Broad diffraction peaks --> plastic deformation (micro-stresses)
4	-225	27	-1113	11				Broad diffraction peaks --> plastic deformation (micro-stresses)
5	-230	24	-247	26				Much narrower peaks --> annealing?
6	-709	18	-1055	7				Broad diffraction peaks --> plastic deformation (micro-stresses)

*Data for E and ν from H. Wawra , Z. Metallkunde 69 (1978) 518-523. Isotropic elastic constants assumed.

Sample 5 shows a very distinct qualitative and quantitative residual stress behaviour. The diffraction peaks of sample 5 are much narrower than those of the other samples, fig. 3. The broader peaks of the other samples are as expected for a severely deformed surface layer, induced by the grinding operation. The sharper peaks of sample 5 indicate that such severely deformed layer has been eliminated by polishing. Simultaneously, the level of residual stresses is significantly lower.

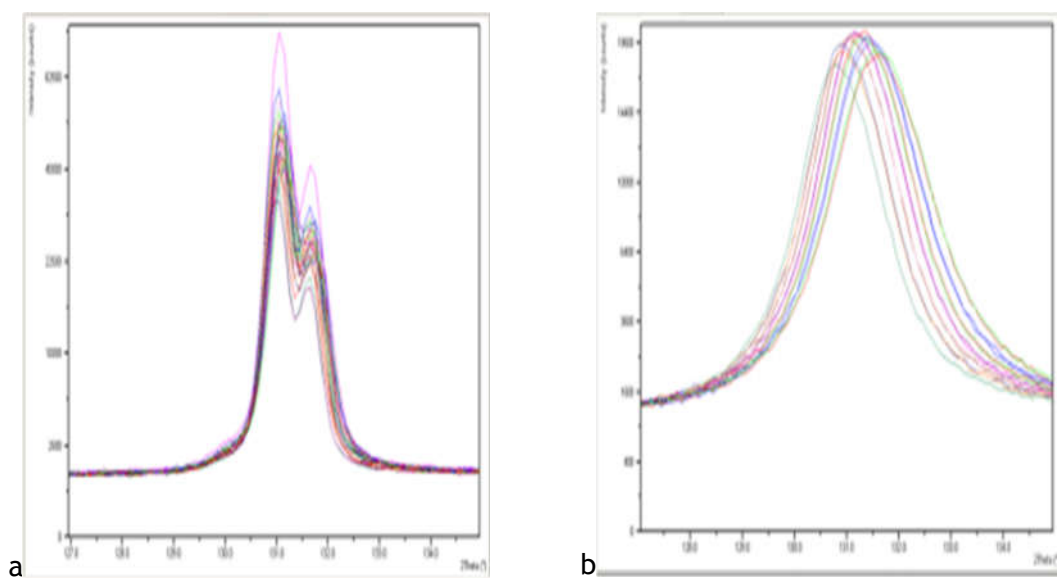


Figure 3. X-rays (321) diffraction peaks, samples 5 (a) and 2 (b).

The different pattern of residual stresses in the surface layer of the bricks can be evidenced by plotting their location in a map of the longitudinal vs. transverse normal stresses in the stress space, fig. 4.

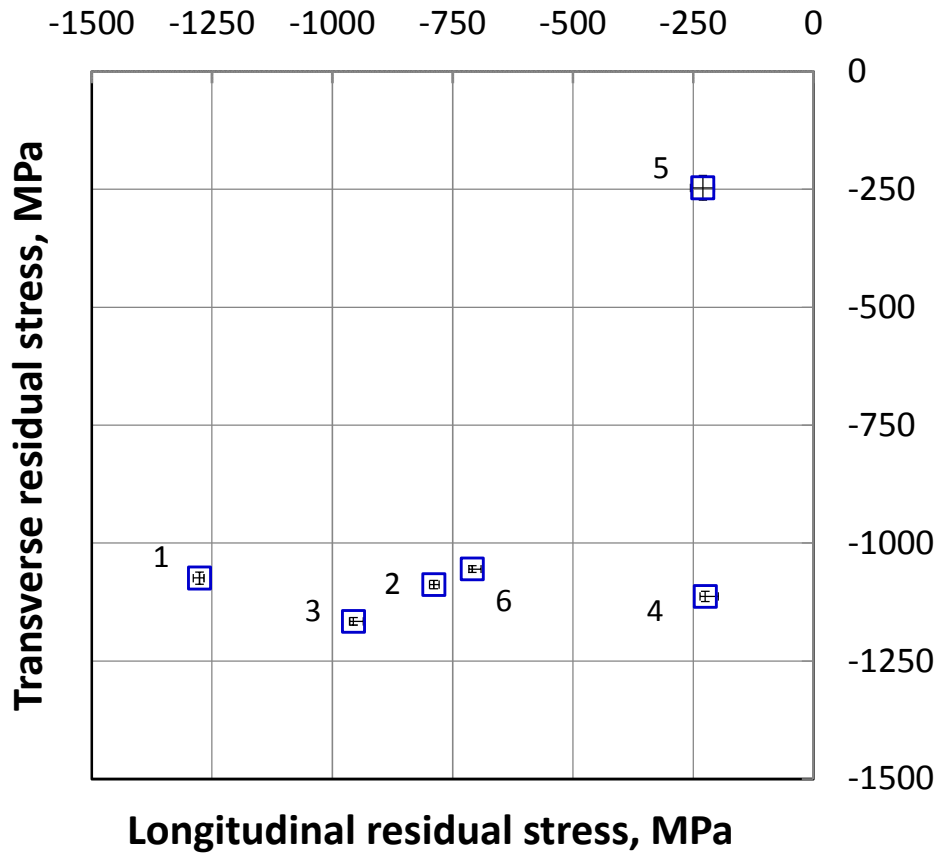


Figure 4. Location of the 6 bricks in a residual stress map of L vs T normal stresses components. Rolling surface, as-received.

2.6 TENSILE STRENGTH AT ROOM TEMPERATURE, L AND T DIRECTIONS

Bending tests at room temperature have been performed using prismatic 2X4X20 mm³ samples in a rig with loading cylinders of 3 mm of diameter and $L = 16$ mm bending span. The displacement rate was 0.3 mm s⁻¹. The tensile surface of the samples was the original surface of bricks (the other surfaces were machined by EDM and a chamfer of about 100 μm was introduced at the edges by gentle manual polishing). The test machine was an INSTRON 8874. The maximum tensile stress at the surface of the specimens is calculated from the maximum applied force in the bending tests, F , according to the linear elastic formula:

$$\sigma_{max} = \frac{3F_{max}L}{2bd^2}$$

where d is the height of the beam and b its thickness.

The observed macroscopic stress-strain behavior was linear elastic before fracture in all cases, i.e., the behavior was macroscopically brittle and the tensile strength measured is a brittle fracture strength. The detailed results are gathered in Table 7. The average values have been represented as an L-T map in fig. 5.

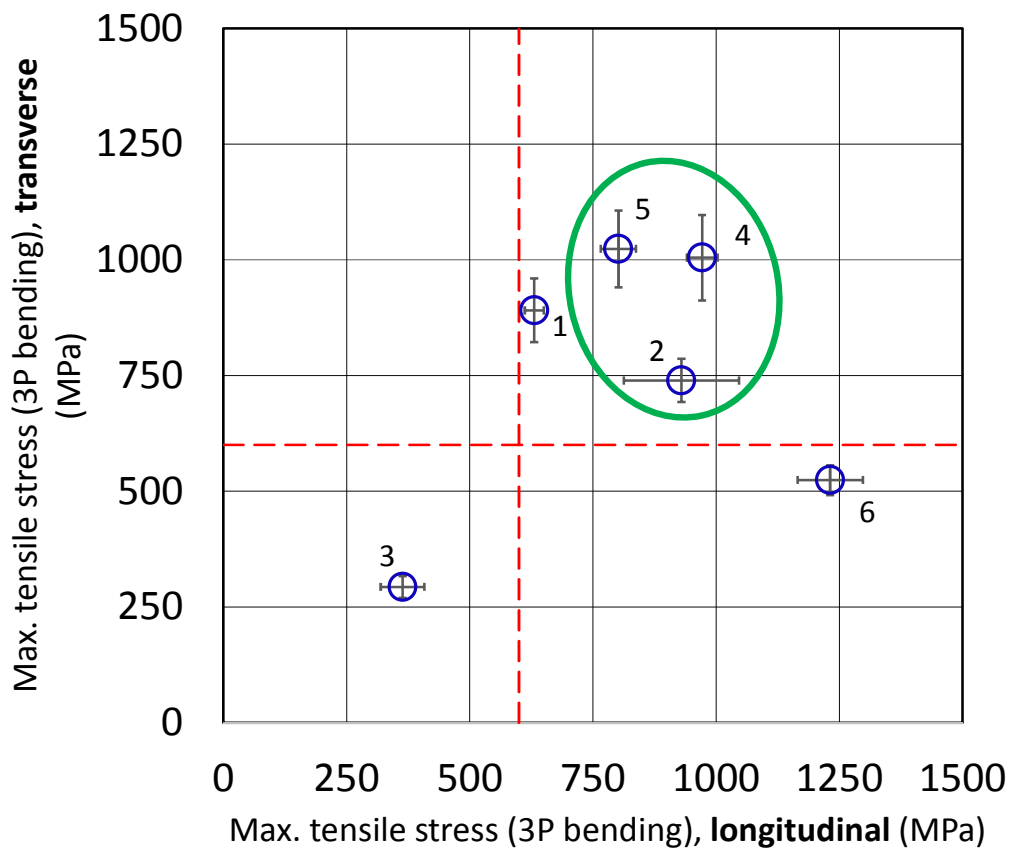


Figure 5. Average tensile strengths (RT) of the 6 batches of bricks. Longitudinal vs. transverse results. The tensile surface was the as-received rolling surface. Red dotted lines mark the 600 MPa limit. Encircled in green, the 3 best batches from this point of view.

- Bricks 3 and 6 fall on the excluded zone according ESS-Bilbao specification in its call for suppliers ($\sigma_{\max} < 600$ MPa).
- Brick 1, inside the allowed zone, but close to the exclusion border.
- Bricks 2, 4 and 5 well inside the allowed zone.
- Bricks 2, 4 and 5 display the best mechanical behavior at room temperature.

If we confront figs 4 and 5, we can conclude that here is no clear relationship between the fracture strength and the residual stresses at the surface. For instance, fracture anisotropy of brick 6 does not appear to be related with internal stress state.

The reasons for the good/bad behavior of the other bricks are to be found in their surface condition and in their structure (in broad sense).

TABLE 7. RESULTS, 3P BENDING TESTS AT ROOM TEMPERATURE

		3P bending tests		Distance between cylinders (3 mm diameter)					
				L=15,97 mm		7,963+8,007 mm			
								Average	St dev p.
Brick	Orient.	spec	b mm	d mm	F_{max} N	σ_{max} MPa	ave Mpa	st p Mpa	
1	L	1	1,985	4,0262	843	627,585	630,8935	19,3745	
		2	2,029	4,021	834	608,9926			
		3	1,99	4,025	883	656,103			
	T	1	1,9632	4,0032	1212	922,8257	890,9801	68,73896	
		2	1,9556	4,0152	1047	795,5152			
		3	1,964	4,0076	1257	954,5996			
2	L	1	1,9782	4,0244	1070	800,0322	929,6523	116,677	
		2	1,9768	4,0262	1212	906,0358			
		3	1,9984	4,038	1473	1082,889			
	T	1	1,9588	4,0228	892	674,0841	739,4639	46,57907	
		2	2,0336	4,024	1071	779,1197			
		3	1,962	4,0204	1013	765,1879			
3	L	1	1,966	4,0294	468	351,2188	363,5164	44,38614	
		2	1,9718	4,0304	423	316,357			
		3	2,0306	4,0324	583	422,9735			
	T	1	1,959	4,0022	390	297,7342	293,2626	23,5264	
		2	1,961	4,002	419	319,5791			
		3	1,983	4,0078	349	262,4743			
4	L	1	2,0342	4,045	1397	1005,453	971,6845	31,5854	
		2	1,9852	4,03	1251	929,478			
		3	1,9912	4,0252	1320	980,1224			
	T	1	1,977	4,0096	1445	1089,069	1004,687	92,13906	
		2	1,9662	4,0068	1155	876,5065			
		3	1,9636	4,01	1382	1048,486			
5	L	1	2,011	3,9834	1050	788,2529	801,7898	35,83958	
		2	1,974	3,9878	1115	850,8581			
		3	1,9714	3,9822	1000	766,2585			
	T	1	1,9562	3,9904	1233	948,2288	1023,502	83,25923	
		2	1,9628	3,9786	1478	1139,552			
		3	2,0368	3,9716	1318	982,7254			
6	L	1	1,9708	4,022	1517	1139,869	1231,33	66,17019	
		2	1,9752	4,0202	1679	1259,913			
		3	2,0252	4,0232	1771	1294,206			
	T	1	1,9612	4,0168	746	564,7454	524,0837	32,19924	
		2	1,9752	4,0166	646,5	486,0002			
		3	1,9624	4,013	688	521,5053			

2.7 FRACTOGRAPHY

Fracture surfaces after bending have been examined by scanning electron microscopy in a SEM Philips XL30.

It is to be remarked that the orientation of the tensile loading direction, L, “rolling direction” or T, “transverse direction”, has been established with reference to the external geometry of the bricks, on the assumption that their longest direction was aligned with the rolling direction and their short-transverse direction was aligned with the transverse rolling direction in the machining of the bricks from a rolled plate. Obviously, however, the machining of the bricks in some cases was perhaps performed with the geometry of the prismatic bricks rotated 90° around the rolling plane normal. The only way to dissipate this doubt is to perform metallographic examinations in two perpendicular sections and by studying the crystallographic texture, both things out of the scope of this stage of the research. This remark is a warning because we have some doubts about the orientation of some of the batches (bricks 1, 4 and 5) after the observation of the orientation degree of the cleavage facets of the fracture surfaces, which reflect the grain structure. Re-locating the position of these bricks in fig. 5 would change somewhat the tensile strength map if the tensile strength was dominated by the structure more than by the surface roughness, fig. 5bis.

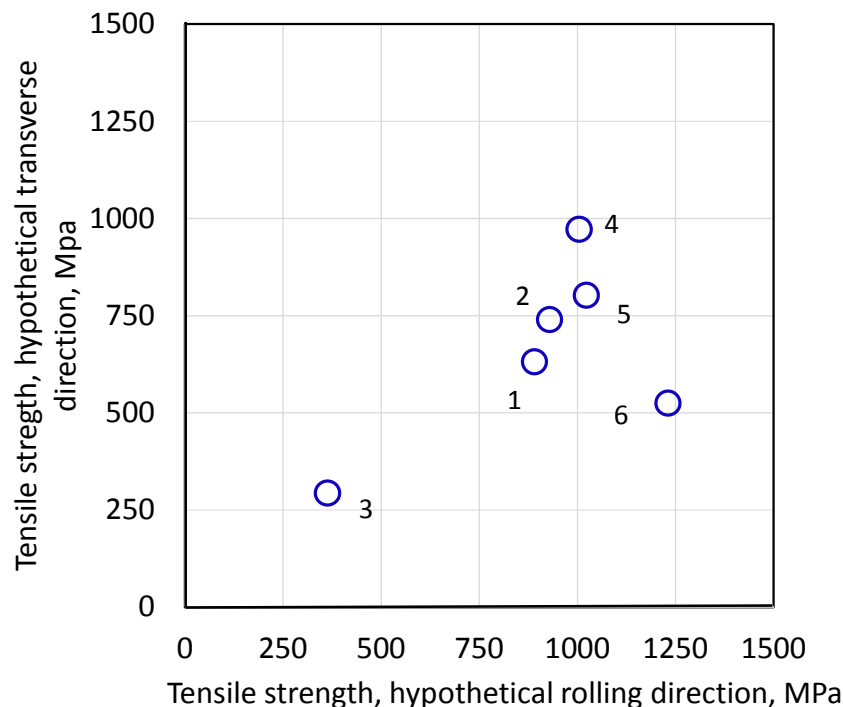


Figure 5bis. Id. Fig. 5 with data 1, 4 and 5 re-located.

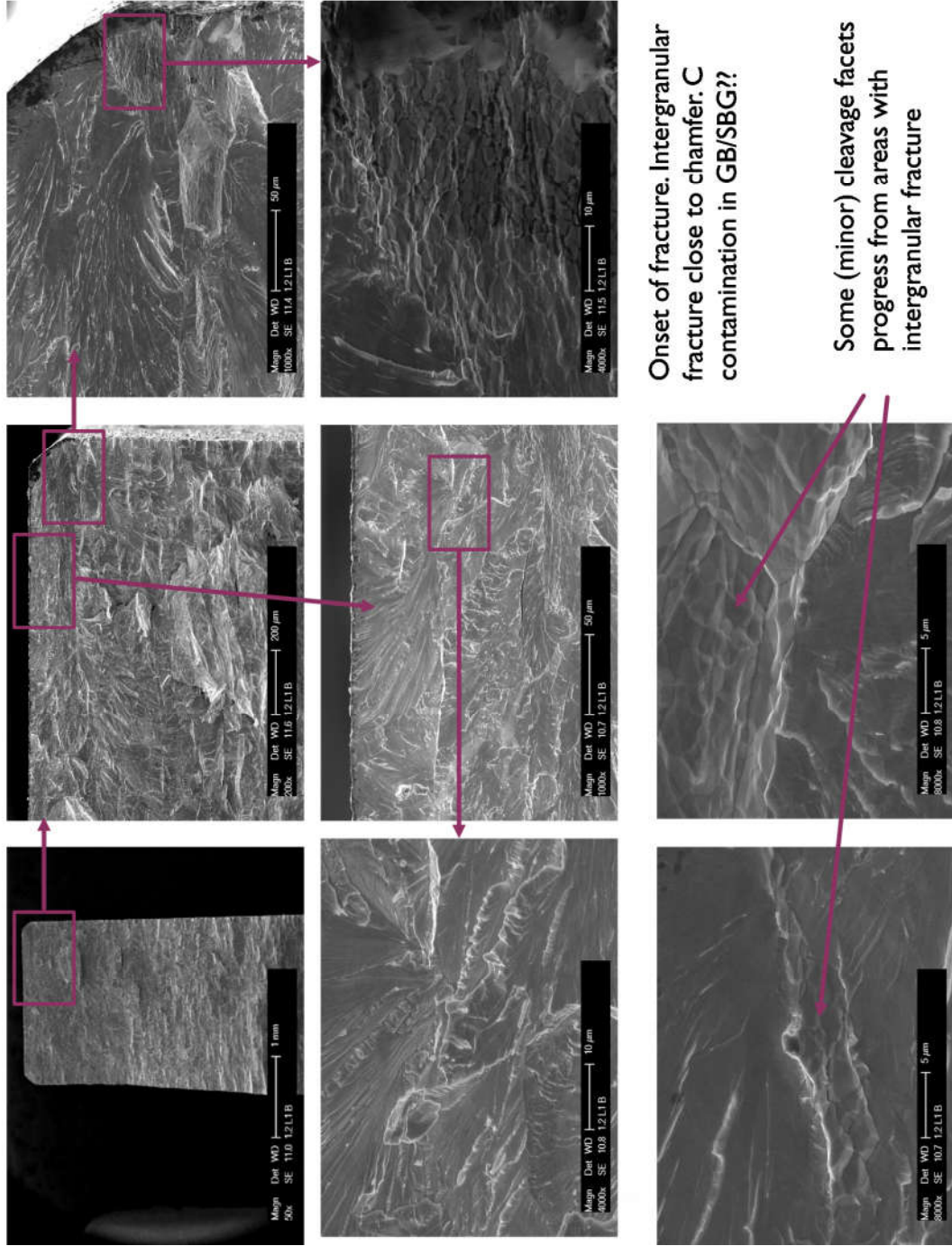
A selection of the fractographic characterization of the 3P bending samples is presented in the following pages, figs. 6-19. Images of larger size of fractures in respectively L and T direction are shown in figs. 20-24 and in figs. 25-29, in order to better appreciate the grain structure.

Brick 3 has an equiaxed, fully recrystallized structure and has failed by intergranular decohesion. It contains a high density of relatively large pores.

The other bricks display a fracture surface dominated by cleavage with the typical distorted pattern of cleavage of a deformed polycrystal. Some regions of intergranular decohesion are also seen. Their porosity is scarce and pores are small; porosity is absent from brick 6 and brick 2 has a higher concentration of pores than bricks 1, 4 or 5, their pores being larger too.

The grain size in the normal direction (i.e., the thickness of the rolled grains) is rather similar for bricks 2, 4 and 5; 1 has the largest size and 6 the smaller of the five (brick 3 excluded from the comparison).

Supplier I. Orientation L Rolling direction \odot Transverse direction \rightarrow



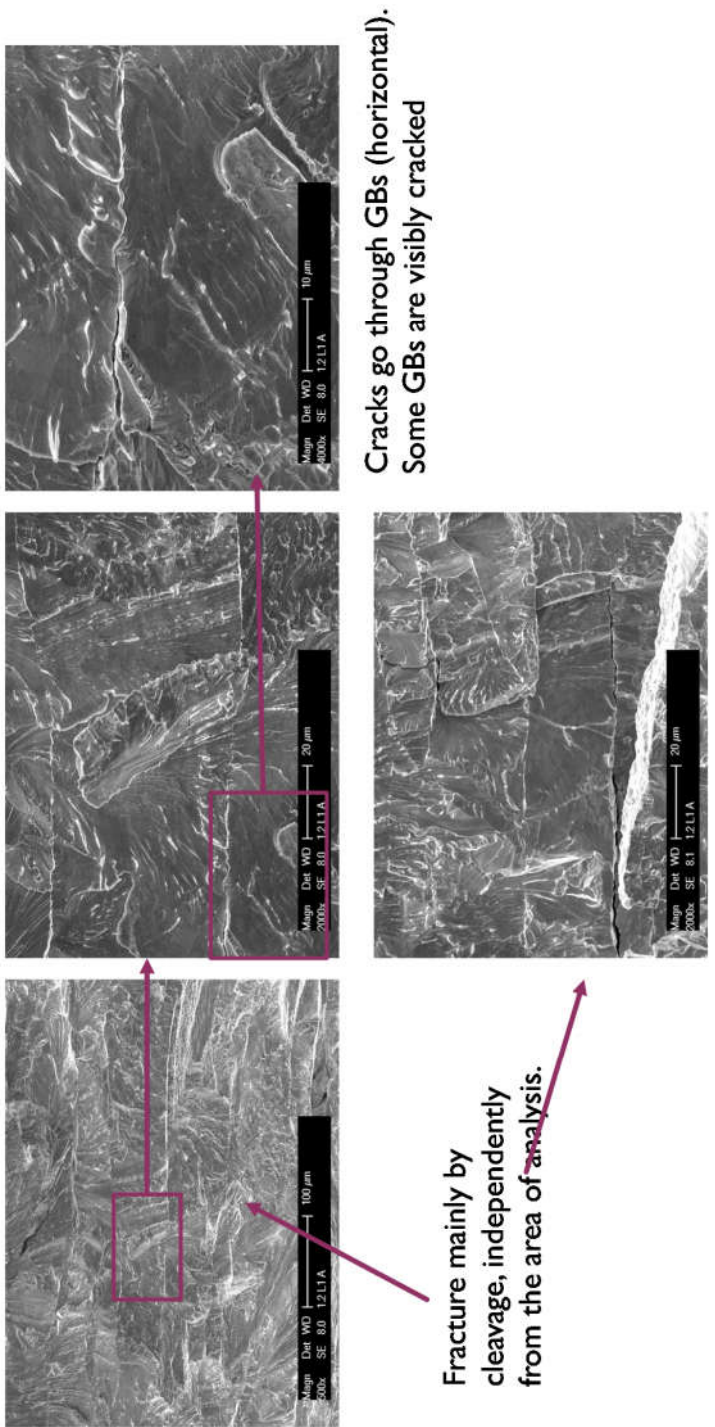
Onset of fracture. Intergranular fracture close to chamfer. C contamination in GB/SBG??

Some (minor) cleavage facets progress from areas with intergranular fracture

Fig. 6

Supplier I. Orientation L. Cont.

Rolling direction → Transverse direction ↻



Cracks go through GBs (horizontal).
Some GBs are visibly cracked

Fracture mainly by cleavage, independently from the area of analysis.

Fig. 7.

Rolling direction →

Supplier I. Orientation T

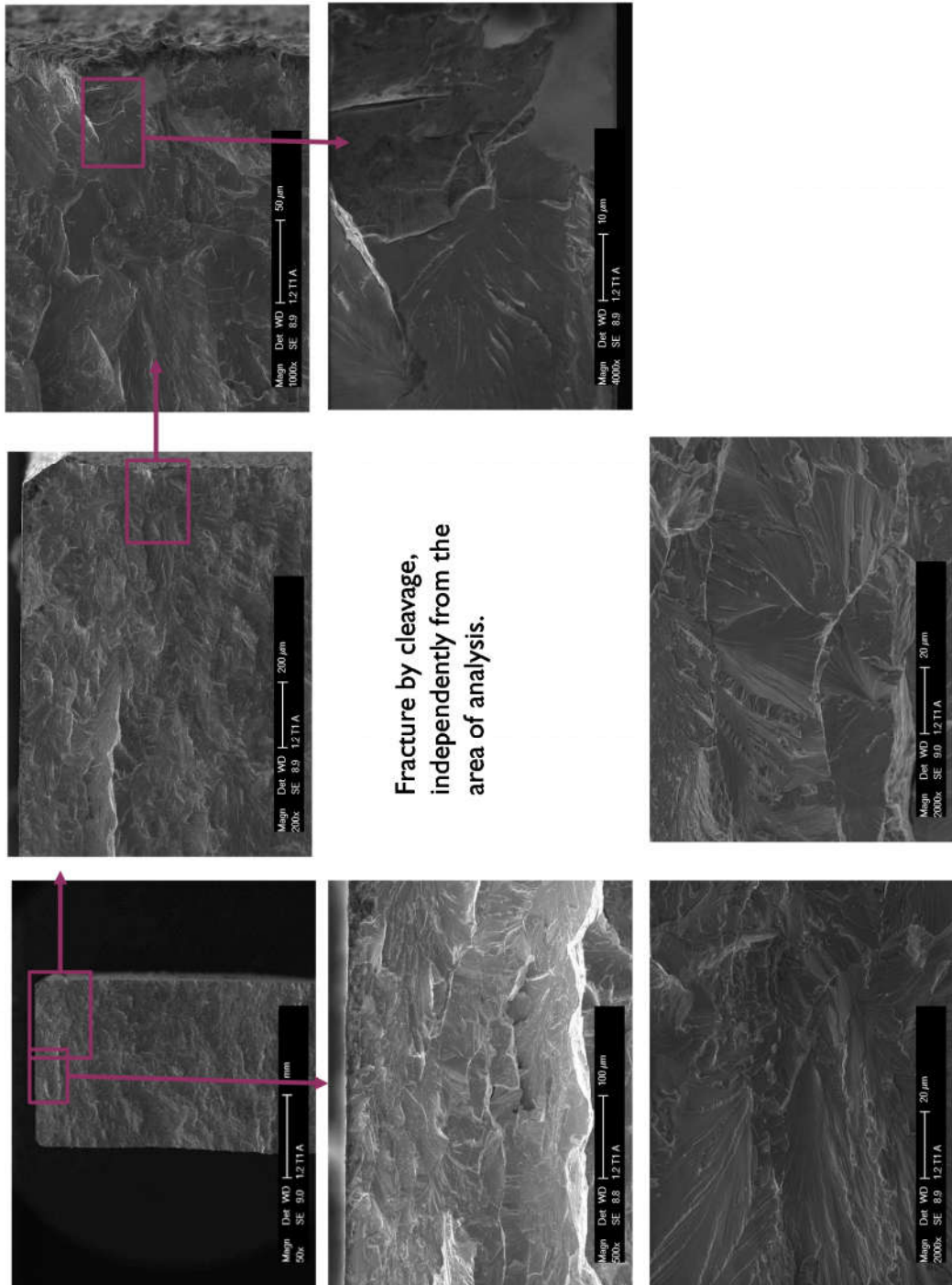
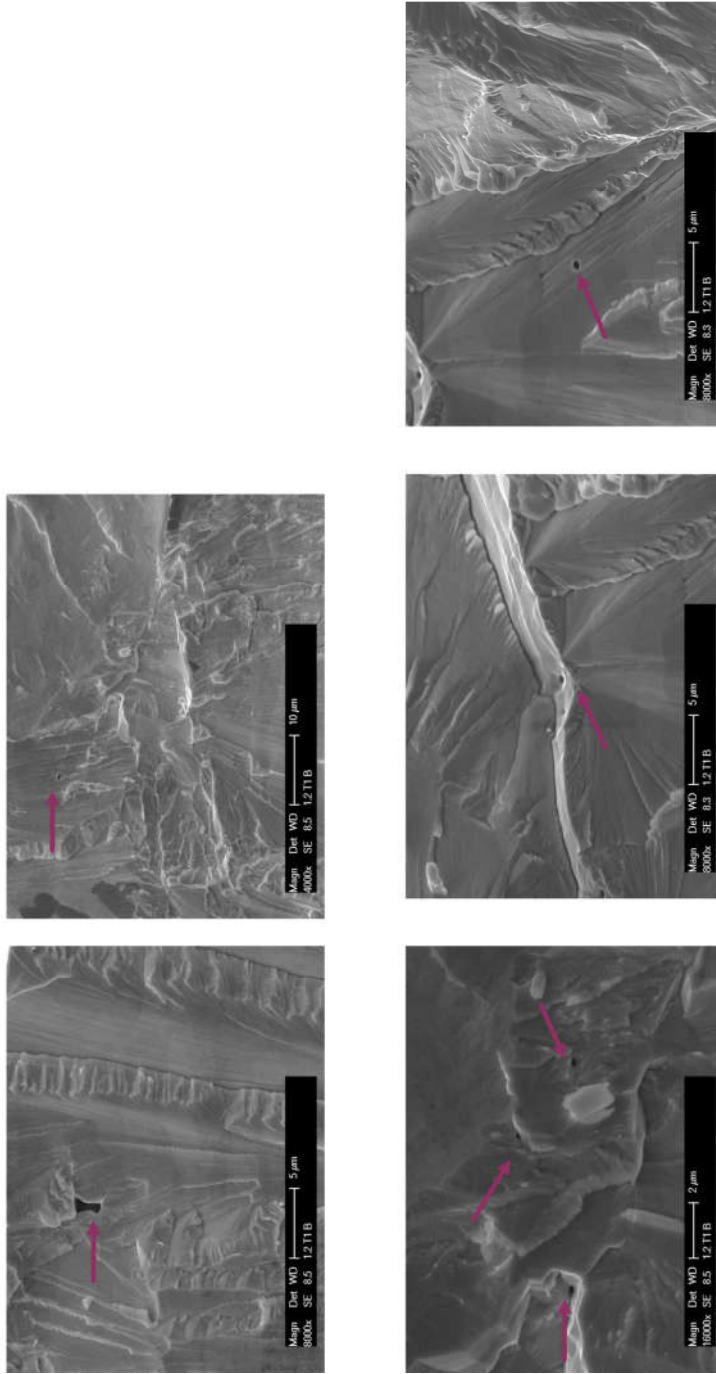


Fig. 8

Rolling direction →

Supplier I. Orientation T. cont



Nanometric pores → some of them stress concentration

Fig. 9

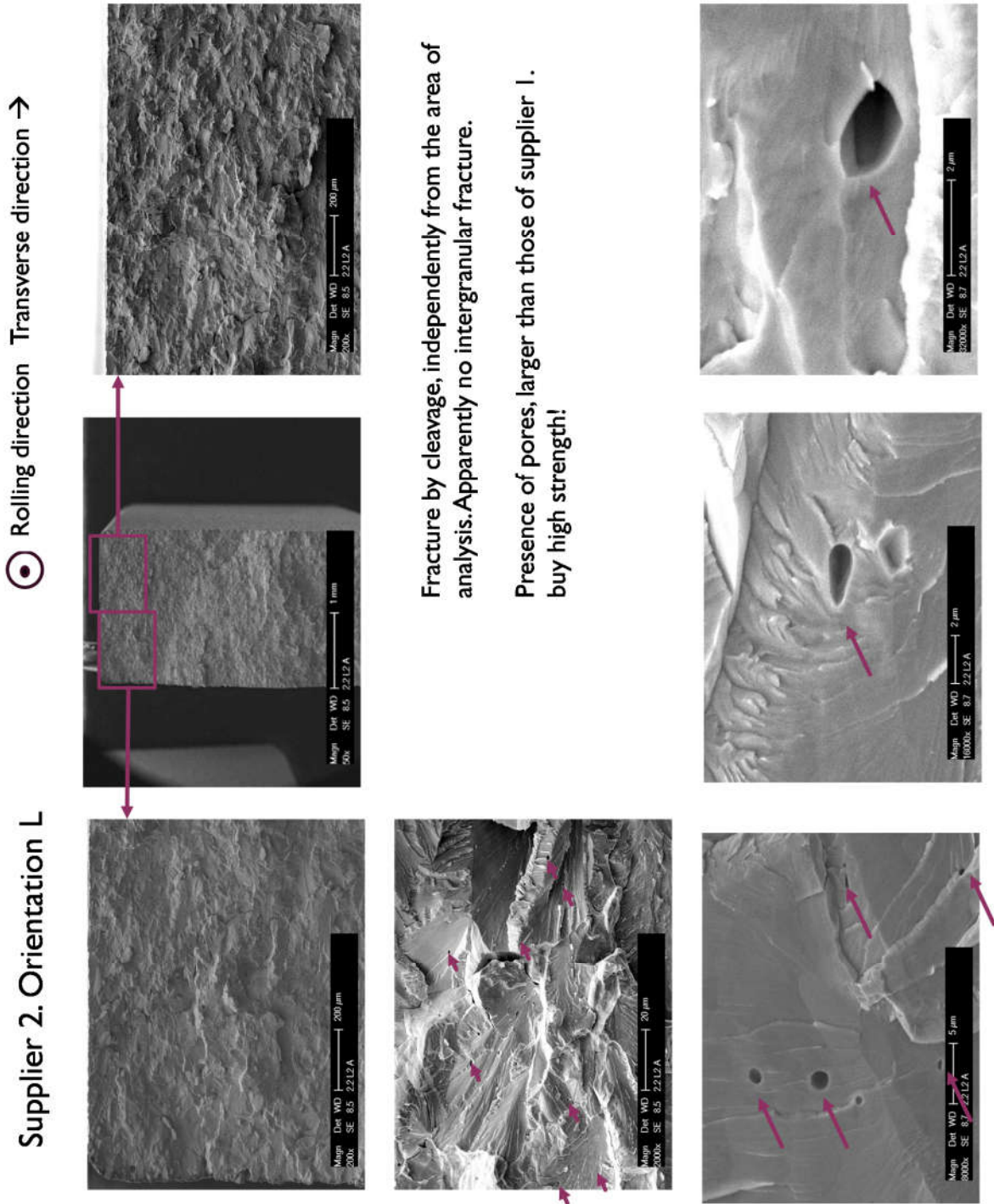
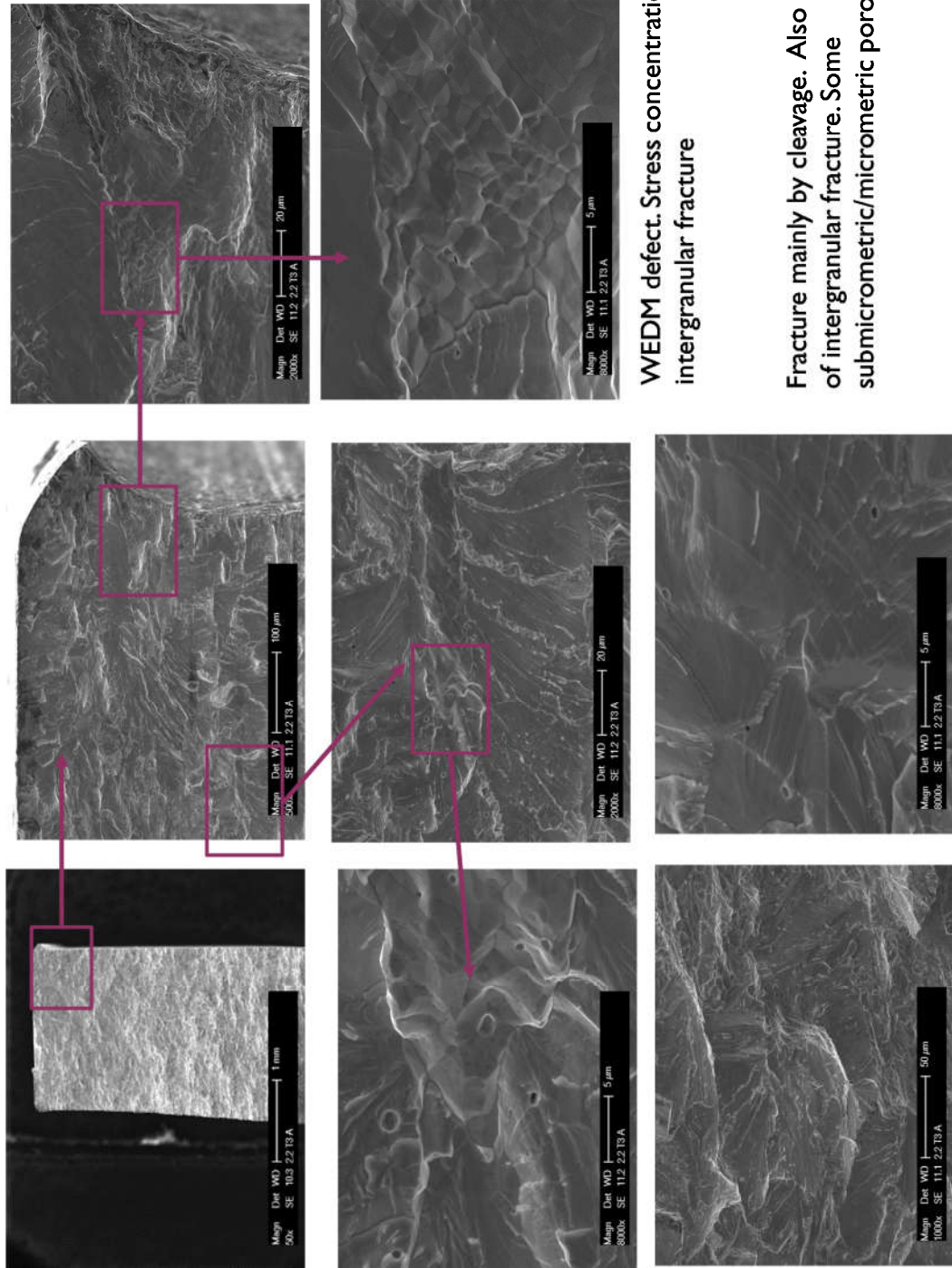


Fig. 10

Supplier 2. Orientation T

→ Rolling direction

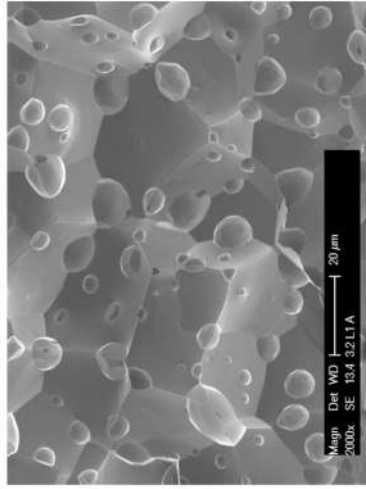


WEDM defect. Stress concentration & intergranular fracture

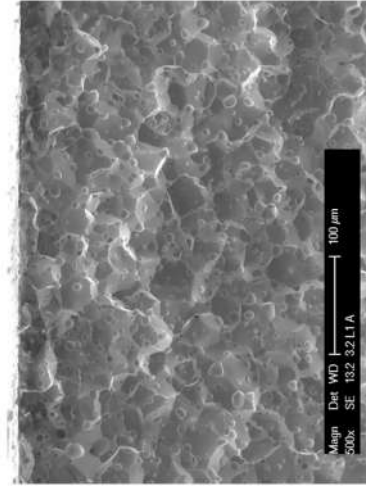
Fracture mainly by cleavage. Also islands of intergranular fracture. Some submicrometric/micrometric porosity?

Fig. 11

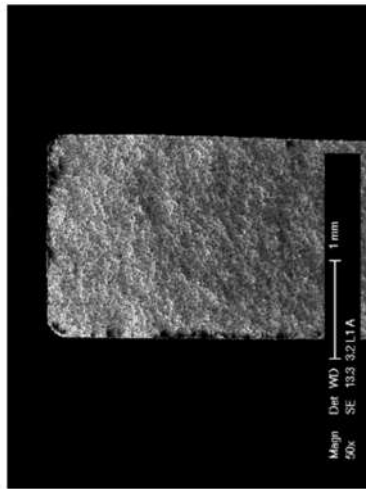
Transverse direction →



Rolling direction



Supplier 3. Orientation L



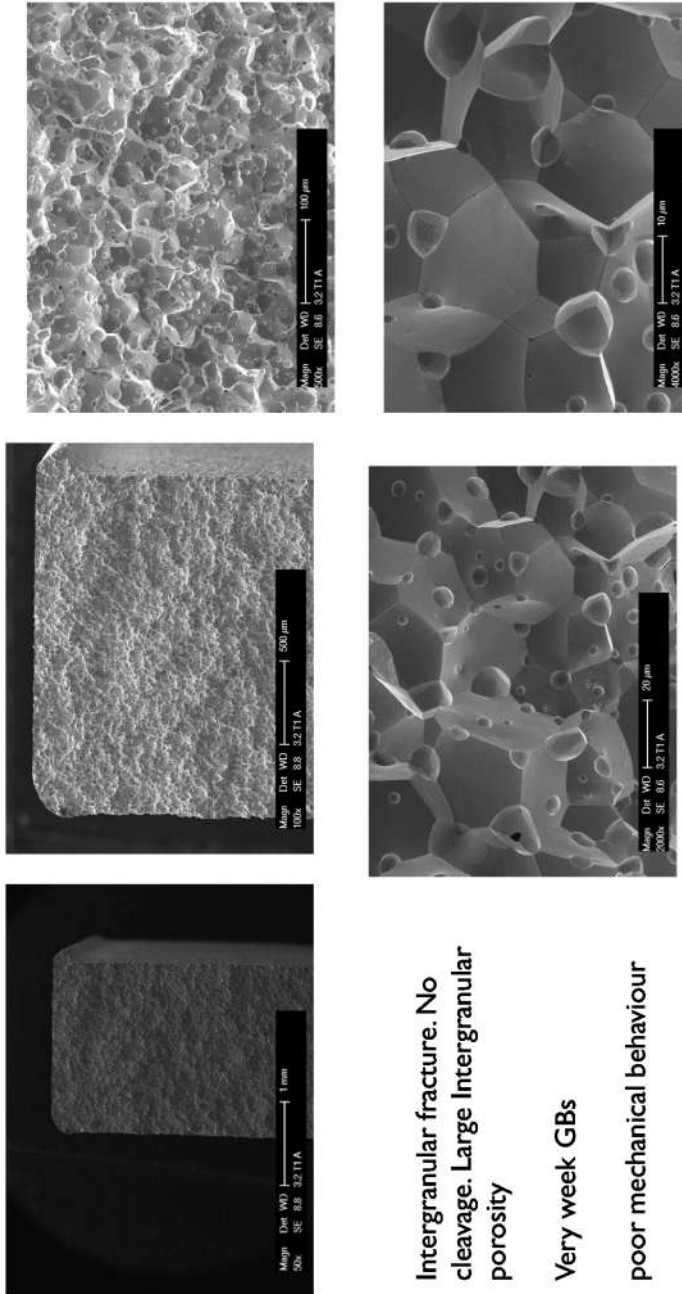
Intergranular fracture. No cleavage.
Large Intergranular porosity

Very weak GBs

Fig. 12

Rolling direction →

Supplier 3. Orientation T



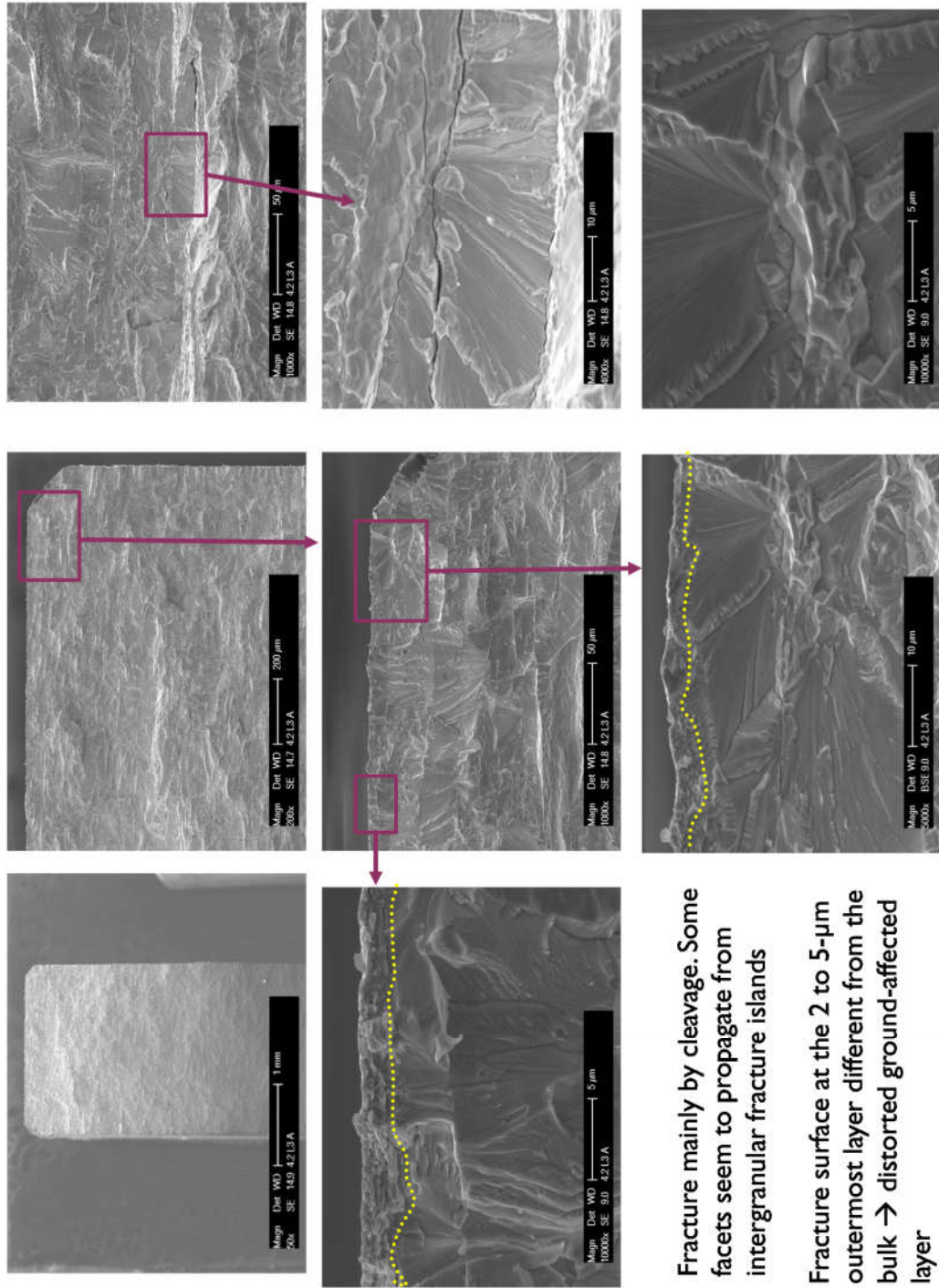
Intergranular fracture. No cleavage. Large intergranular porosity
 Very weak GBs
 poor mechanical behaviour

Fig. 13

Supplier 4. Orientation L

Rolling direction →

Transverse direction →



Fracture mainly by cleavage. Some facets seem to propagate from intergranular fracture islands

Fracture surface at the 2 to 5- μm outermost layer different from the bulk \rightarrow distorted ground-affected layer

Fig. 14

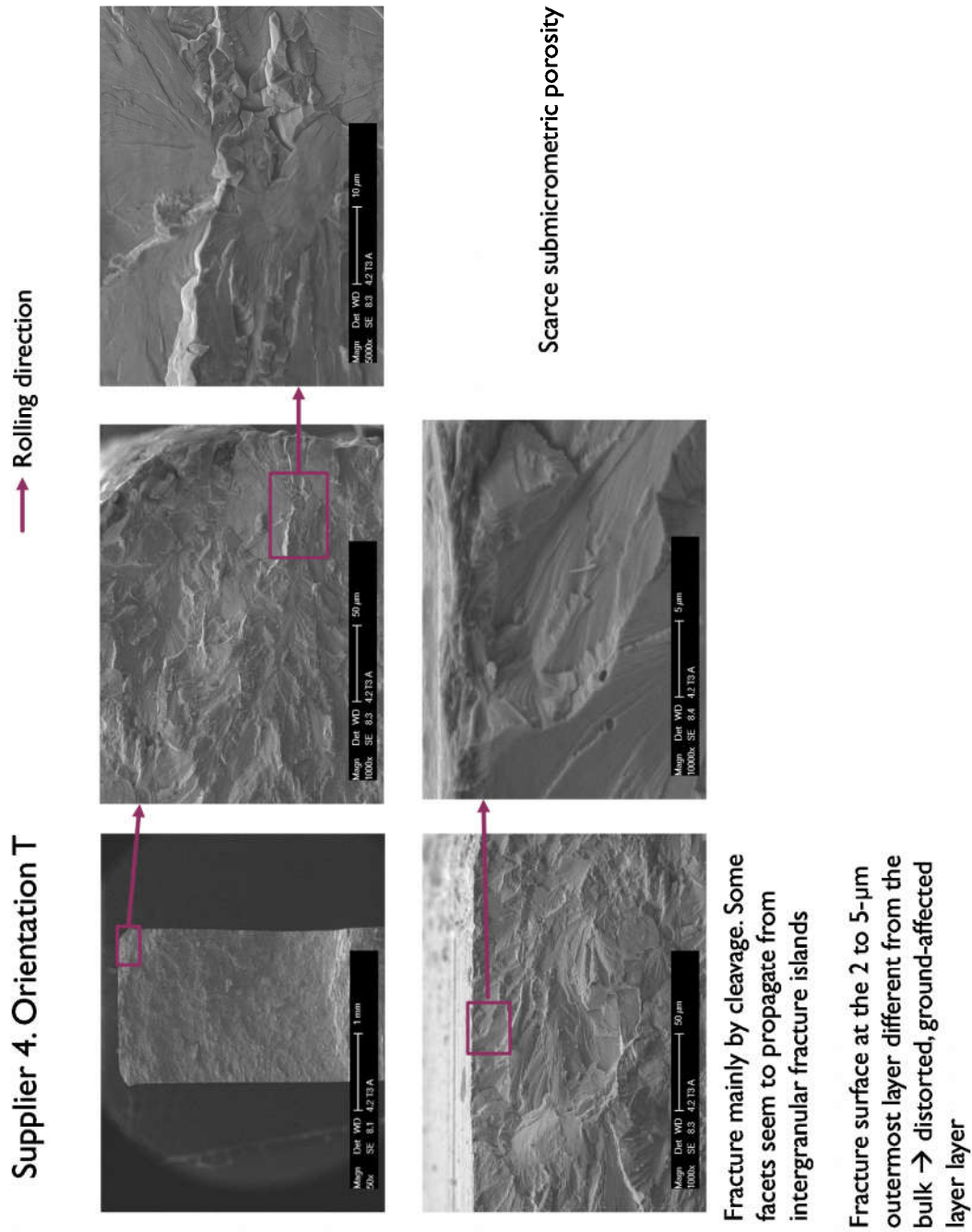
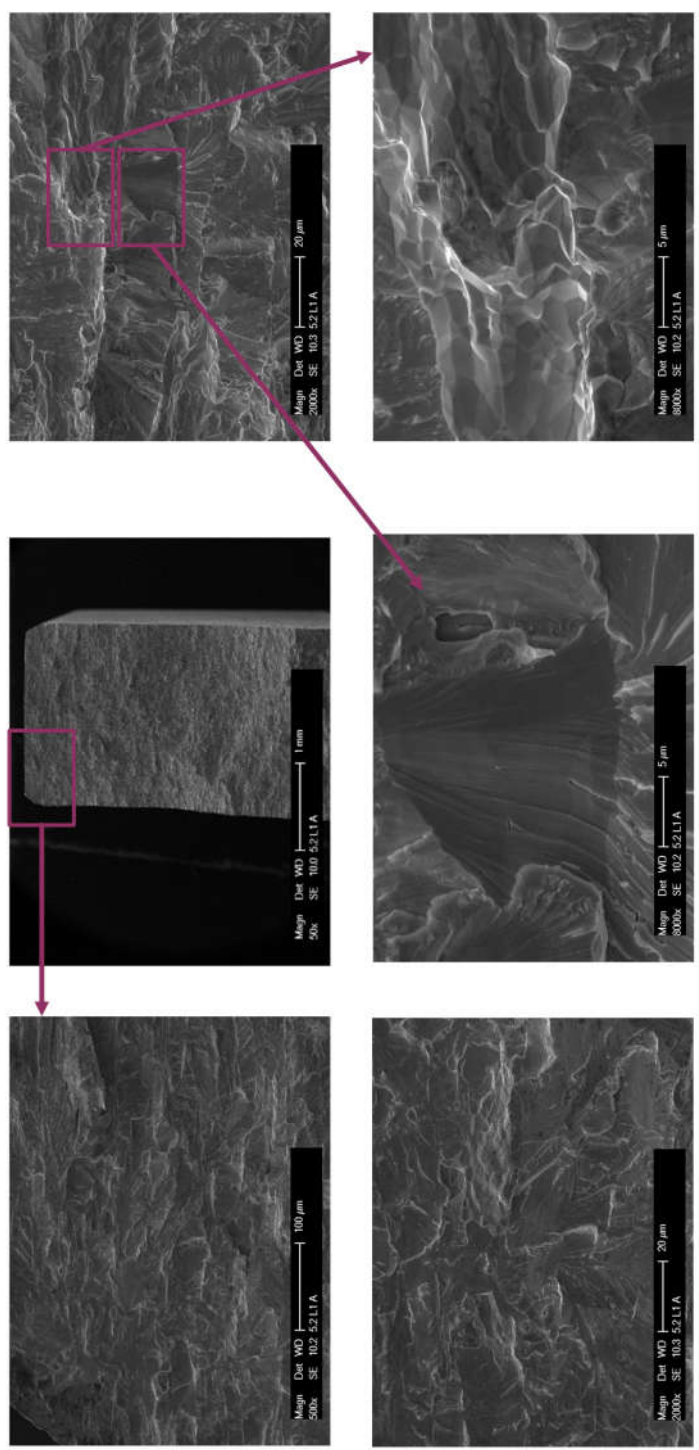


Fig. 15

Supplier 5. Orientation L
Rolling direction → Transverse direction →

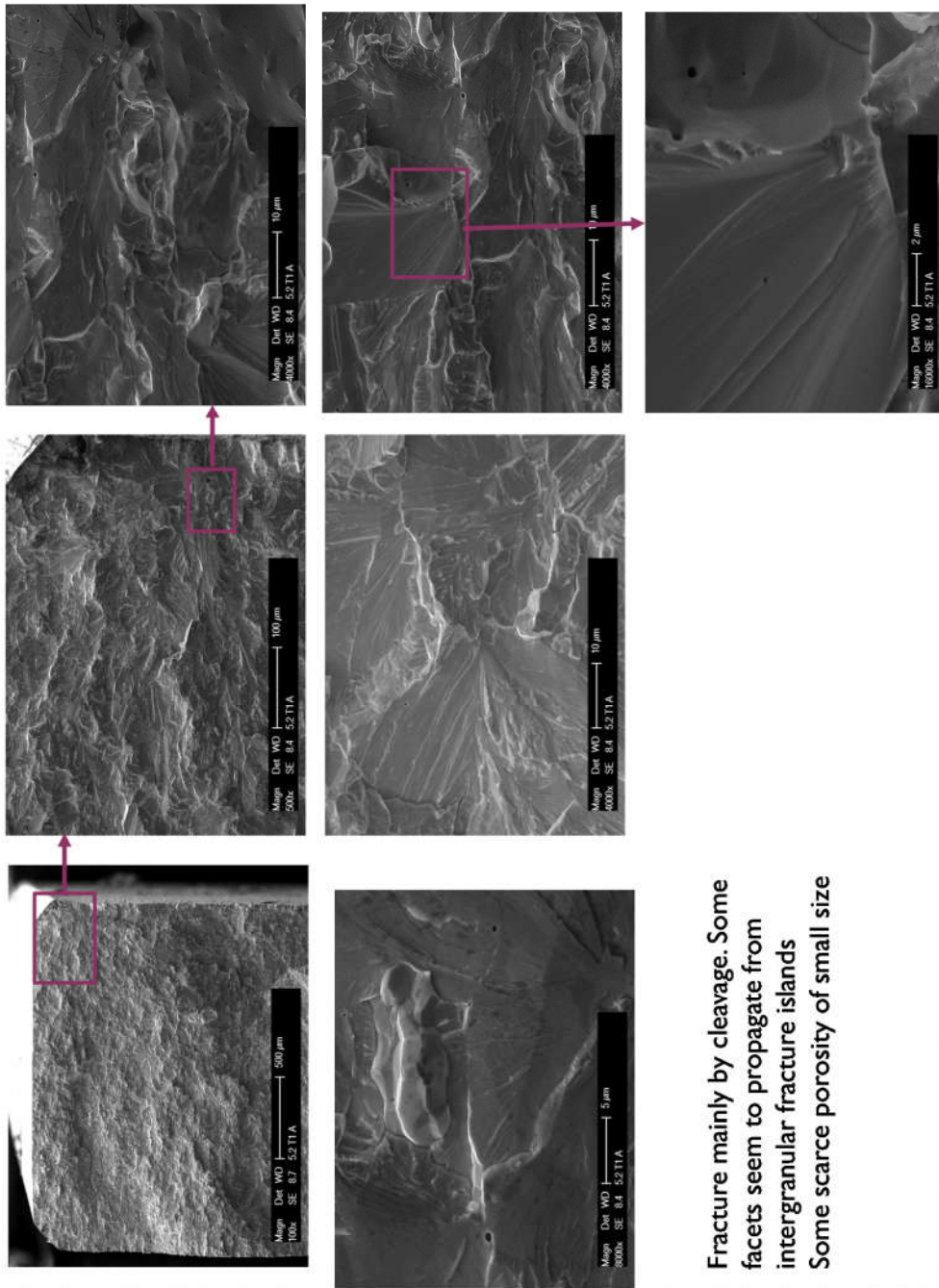


Fracture mainly by cleavage. Some facets seem to propagate from intergranular fracture islands

Fig. 16

→ Rolling direction

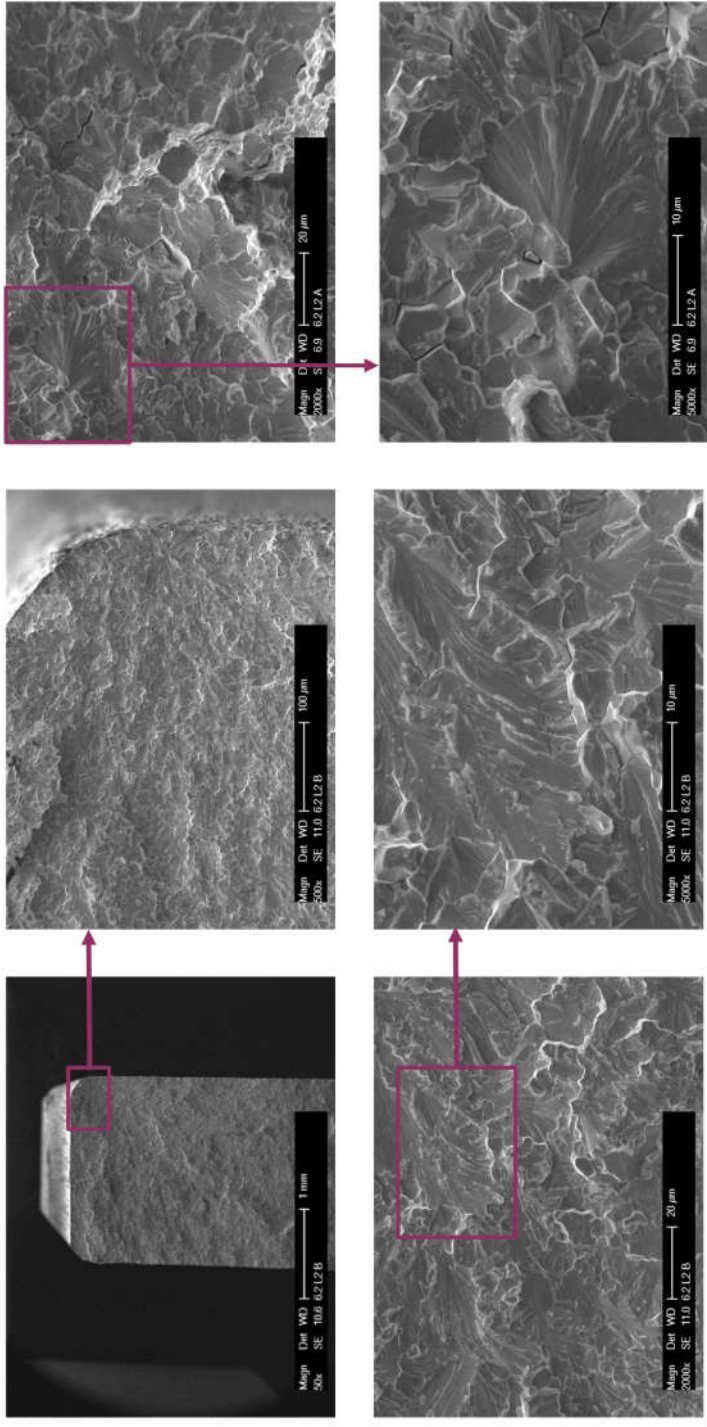
Supplier 5. Orientation T



Fracture mainly by cleavage. Some facets seem to propagate from intergranular fracture islands. Some scarce porosity of small size.

Fig. 17

Supplier 6. Orientation L
Rolling direction → Transverse direction →



Cohexistence of cleavage and intergranular fracture.
Small cleavage facets and intergranular islands

Fig. 18

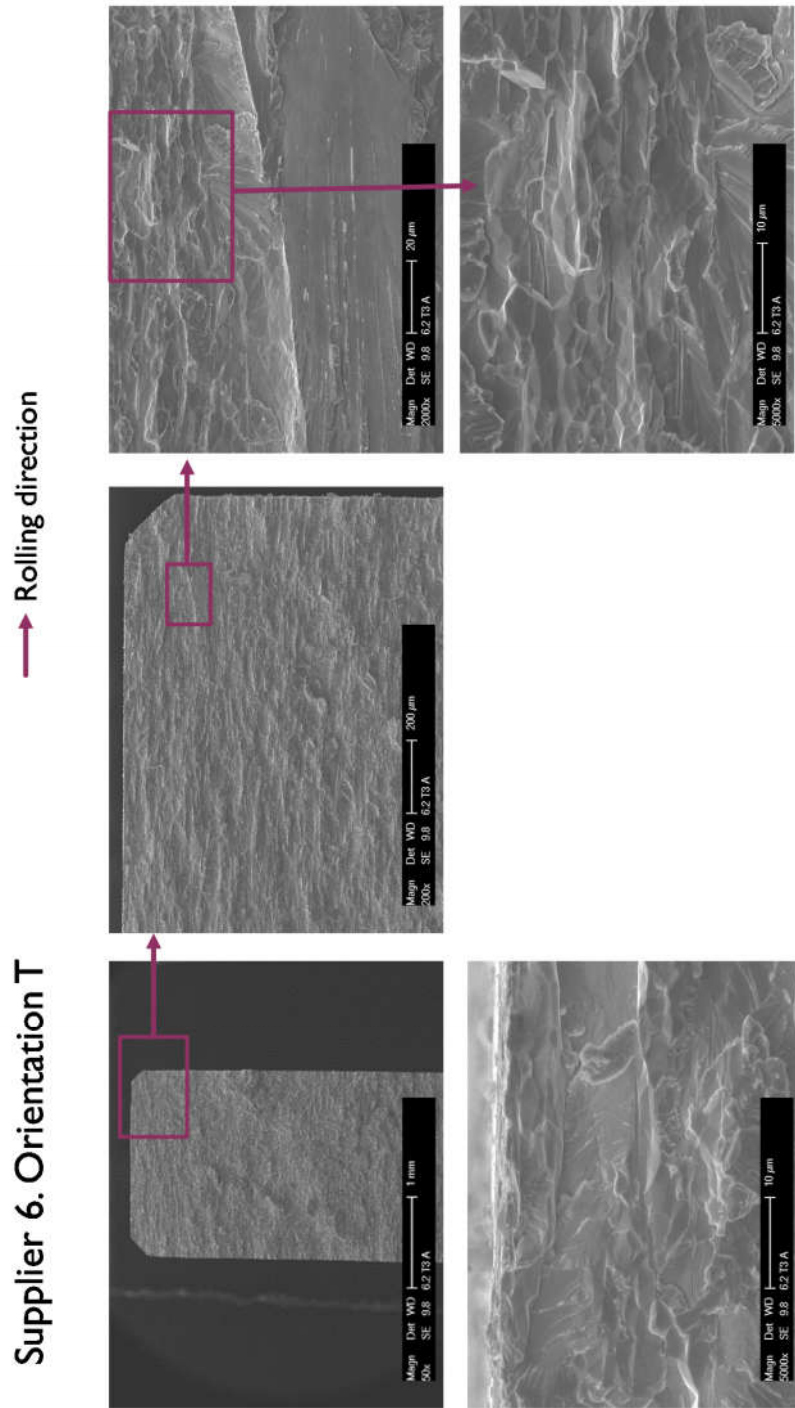


Fig. 19

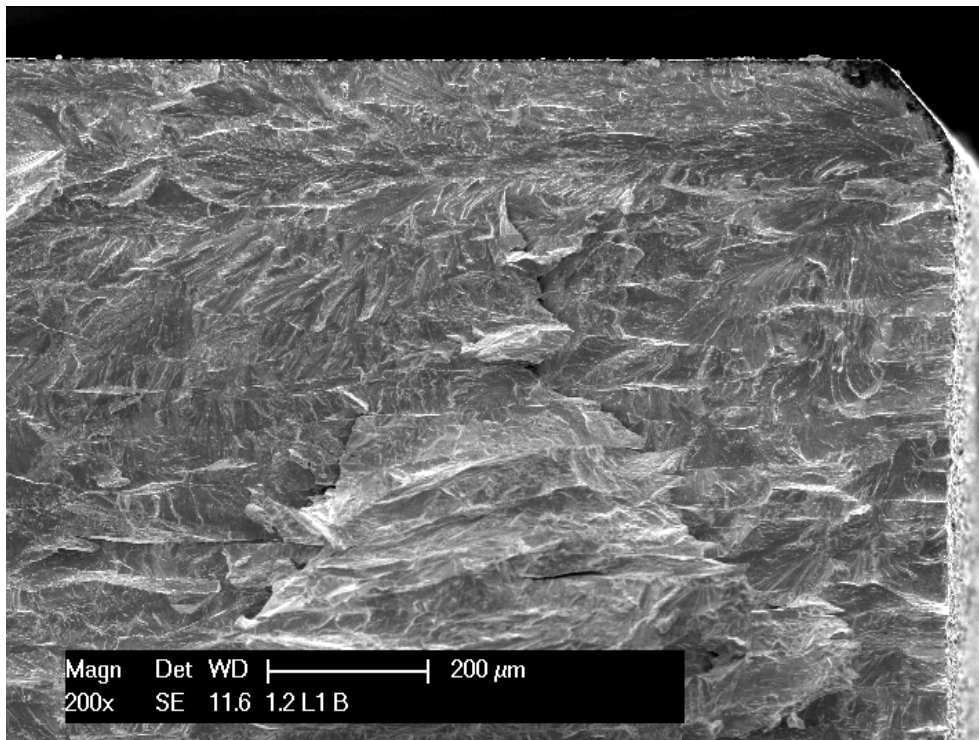


Figure 20. 1, L, x200. Horizontal direction is the presumed transverse-to-the rolling direction.

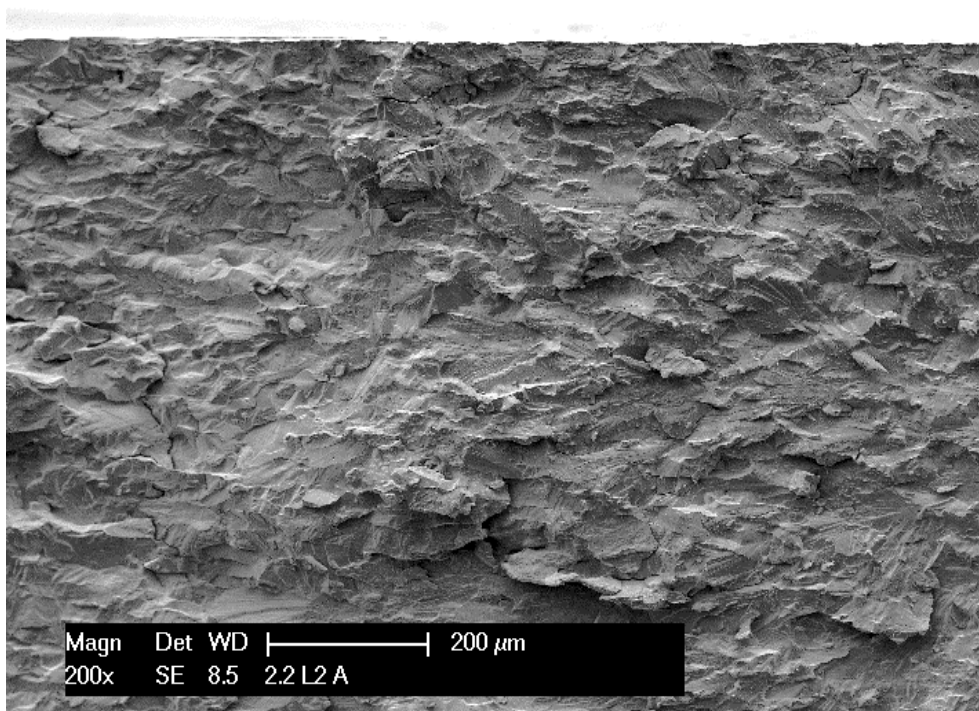


Figure 21. 2, L, x200

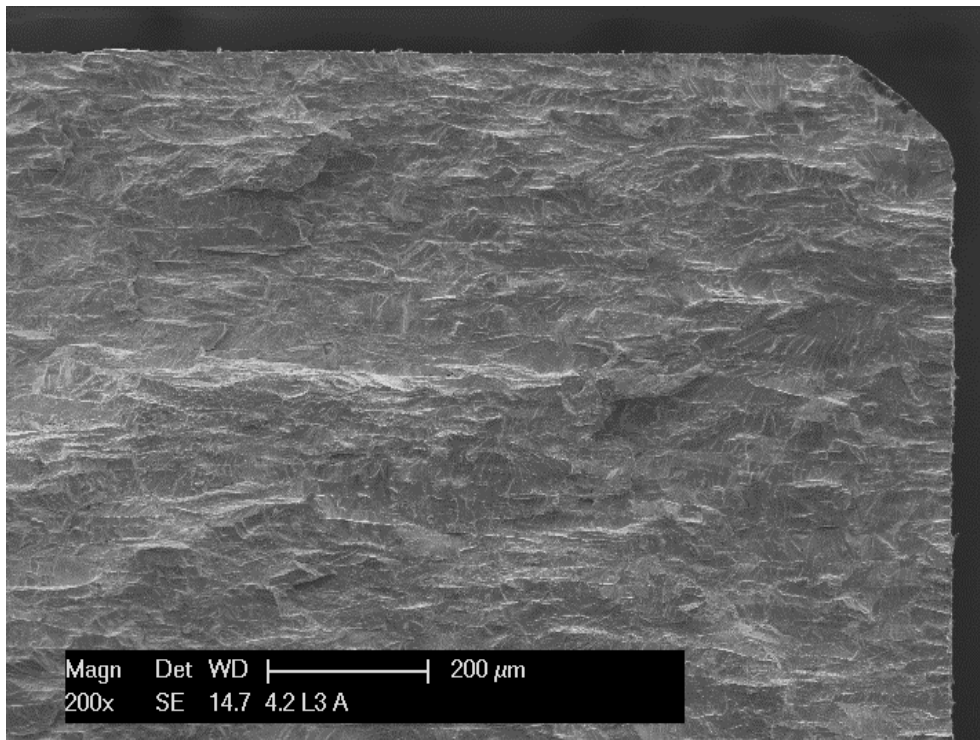


Figure 22. 4, L, X200

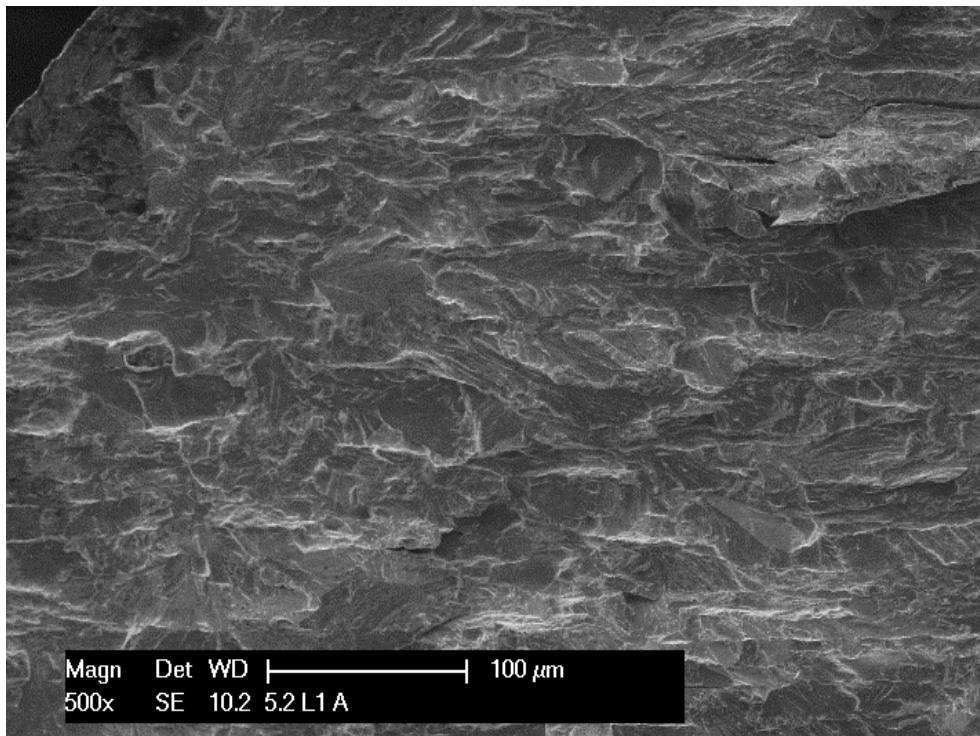
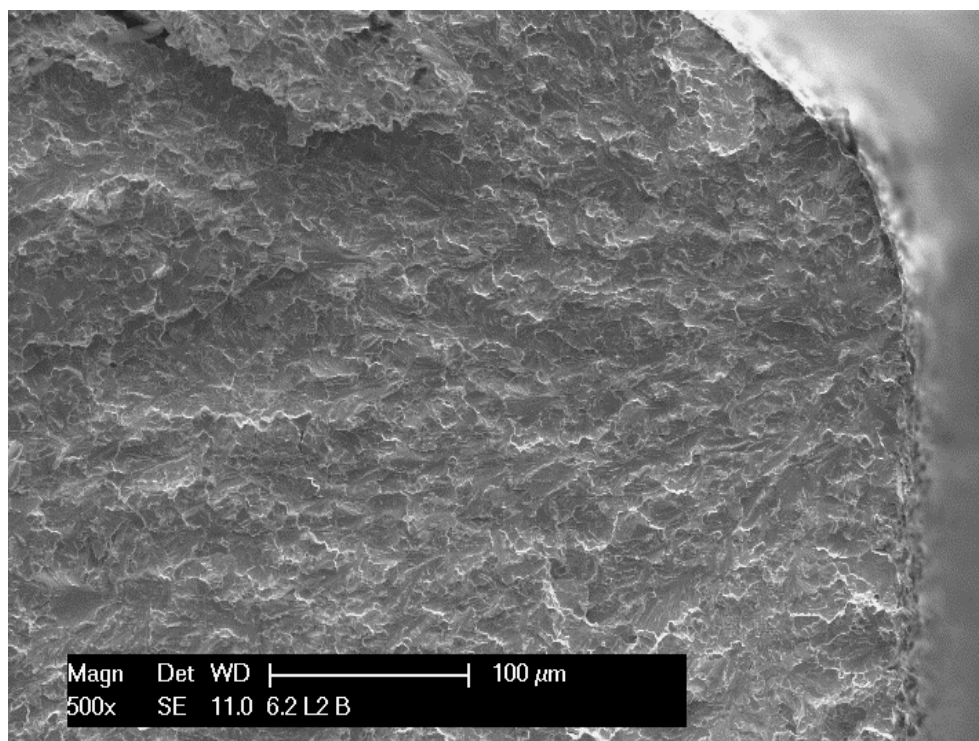


Figure 23. 5, L, x500



Magn	Det	WD		100 μ m
500x	SE	11.0 6.2 L2 B		

Figure 24. 6, L, x500

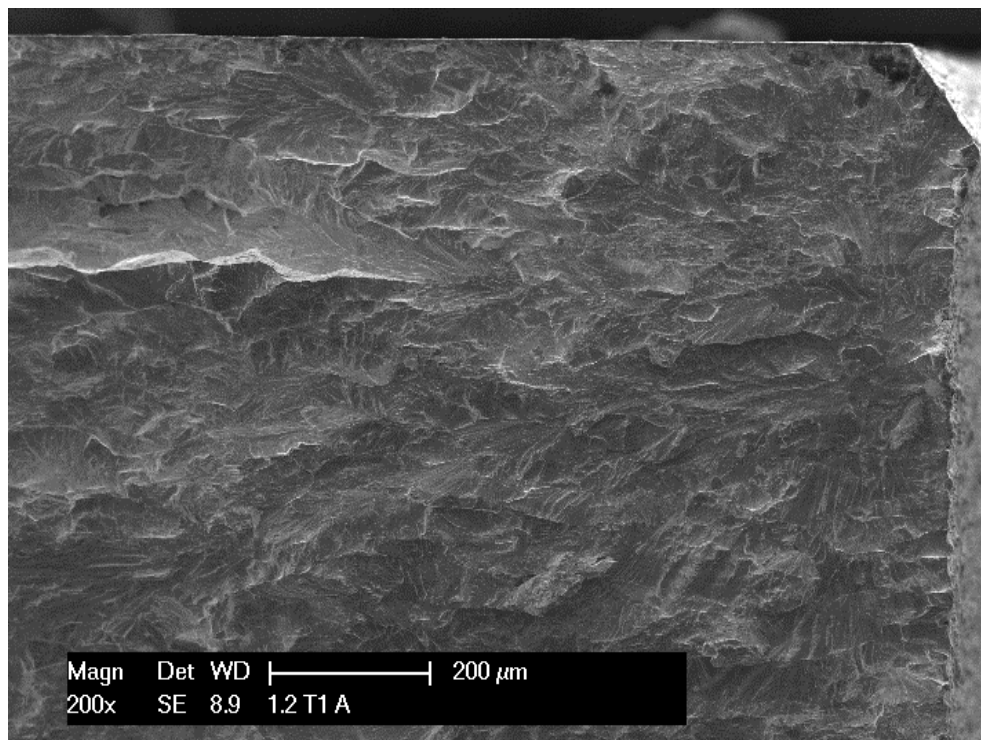


Figure 25. 1 T, x200. Horizontal direction is allegedly, the Rolling direction.

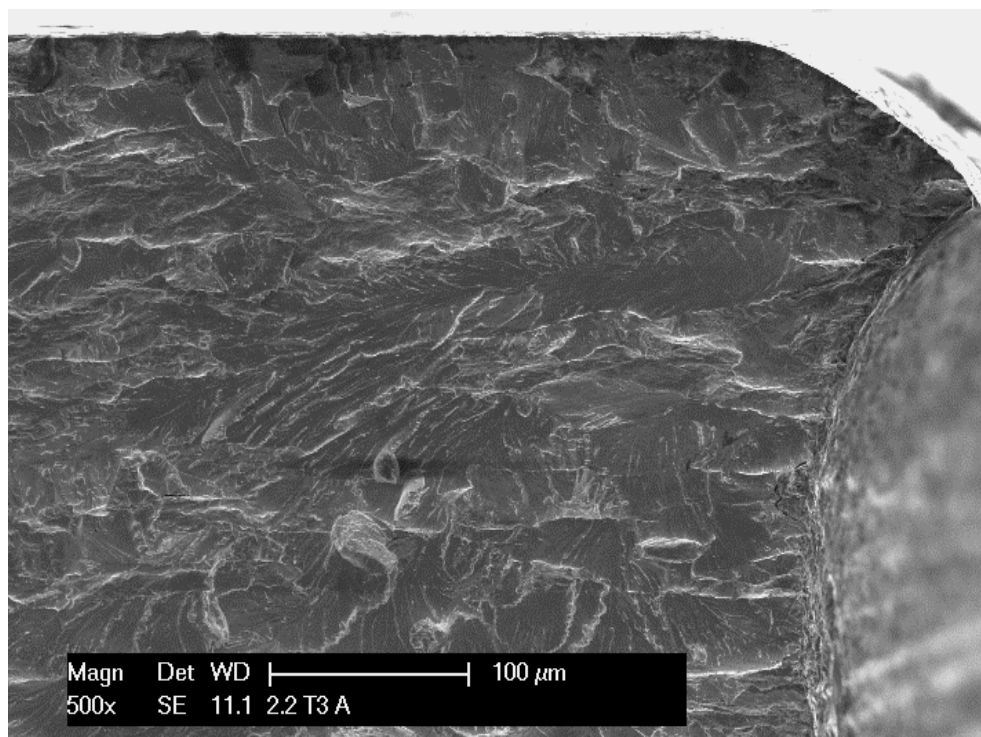


Figure 26. 2T, x500. Edge of the sample. Notice the distorted layer of about 50 mm and the plasticity at the corner, where the plane strain constraint is relaxed.

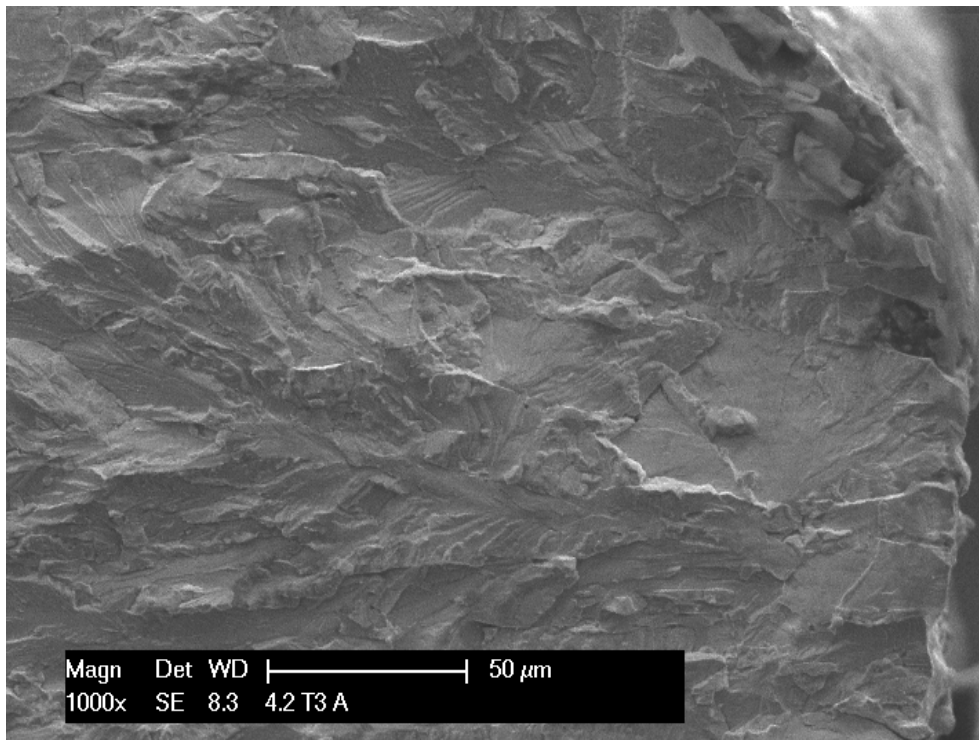


Figure 27. 4T, x1000.

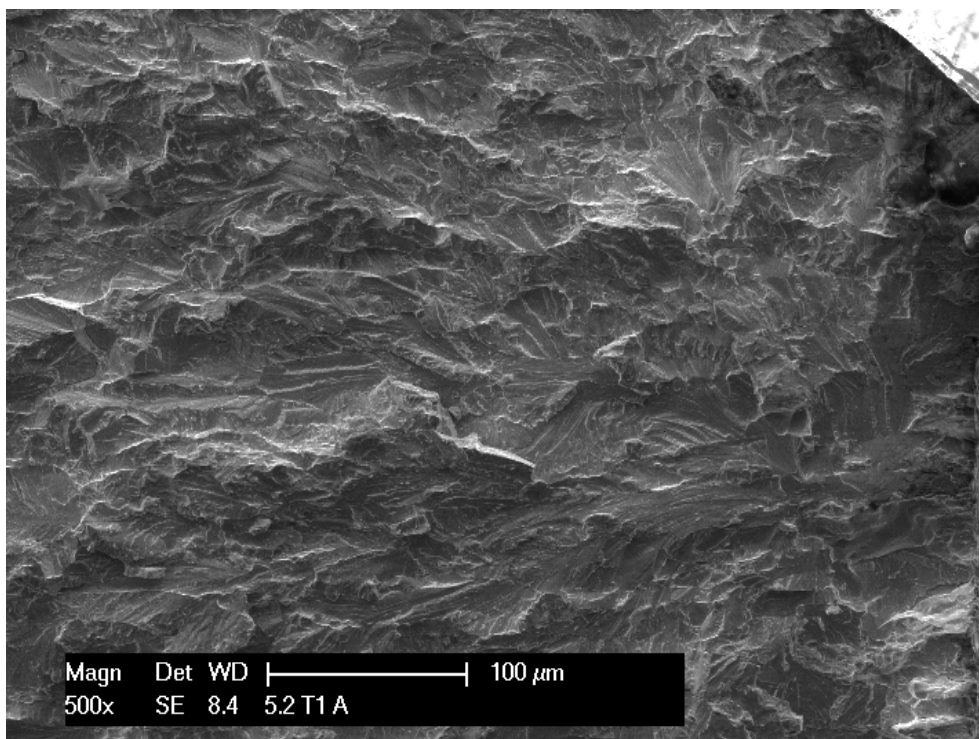


Figure 28. 5T, x500.

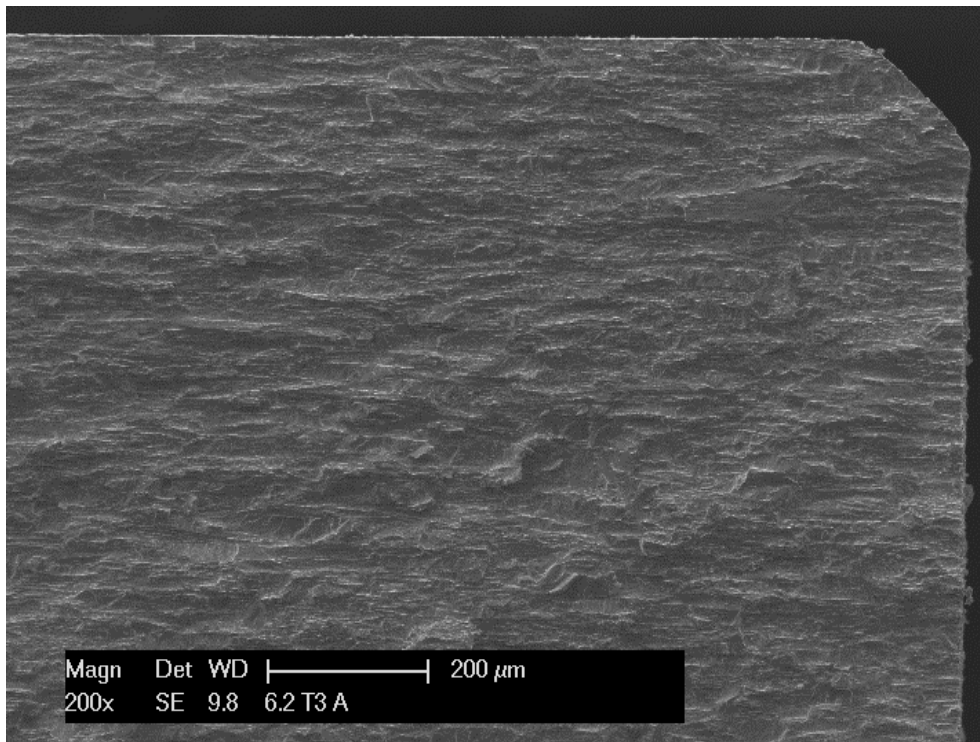


Figure 29. 6T, x200.

3 SUMMARY AND FINAL COMMENTS

TABLE 8. SUMMARY OF RESULTS

W supplier	Visual inspection	Density, ρ (g cm ⁻³)		E, Young modulus RPN (GPa) \pm assoc. error	HV (1 kg) RP (kg mm ⁻²) \pm 95% cl	Res. stresses, surface (MPa) \pm sd		Fractography	Chemical composition Impurities above threshold
		Geom. \pm assoc. error	Water displ. \pm sd			σ_{11} (LD)	σ_{22} (TD)		
1	Grey spots (oxide) on surface	19.22 \pm 0.03	18.95 \pm 0.22	403.9 \pm 0.7	423.7 \pm 25.7	-1276 \pm 9	-1074 \pm 13	Brittle, <u>transgranular</u> , <u>distorted cleavage</u> , <u>oriented facets</u> Minor intergranular fraction Scarce nano-porosity	-
2	Thin continuous (oxide) layer on surface	19.16 \pm 0.03	19.21 \pm 0.03	405.9 \pm 0.8	496.5 \pm 9.5	-789 \pm 11	-1088 \pm 9	Brittle, <u>transgranular</u> , <u>distorted cleavage</u> , <u>oriented facets</u> Minor intergranular fraction <u>Some micro-porosity</u>	-
3	Damaged edges. Scratches on surface, slightly oxidized (finger prints).	18.27 \pm 0.03	17.69 \pm 0.03	364.9 \pm 0.7	355 \pm 6	-956 \pm 20	-1166 \pm 8	Brittle, <u>intergranular fracture</u> , <u>equiaxed grains</u> , <u>high porosity</u> Some prec. at grain edges	-
4	Bright smooth surface, free from oxides	19.24 \pm 0.03	19.20 \pm 0.03	408.1 \pm 0.8	496 \pm 6.0	-225 \pm 27	-1113 \pm 11	Brittle, <u>transgranular</u> , <u>distorted cleavage</u> , <u>oriented facets</u> Minor intergranular fraction Scarce nano-porosity	-
5	Brightest, smoothest surface. Free from oxides	19.22 \pm 0.03	19.23 \pm 0.01	406.4 \pm 0.8	412 \pm 16	-230 \pm 24	-247 \pm 26	Brittle, <u>transgranular</u> , <u>distorted cleavage</u> , <u>oriented facets</u> Minor intergranular fraction Scarce nano-porosity	>30 ppm O (44 ppm)
6	Rough surface, free from oxides. Bricks slightly shorter?	19.26 \pm 0.03	19.15 \pm 0.05	391.4 \pm 0.7	470 \pm 5.0	-709 \pm 18	-1055 \pm 7	Brittle, <u>transgranular</u> , <u>distorted cleavage</u> , <u>oriented facets</u> Minor intergranular fraction Porosity not detected	-

Final comments:

- The brittle behavior of brick 3 is related to a fully intergranular fracture of its recrystallized structure (evidenced by fractography and by its Vickers hardness, much smaller than the hardness of the other samples). Moreover, it has an important porosity, as attested by its poor density and directly evidenced in its fractography. Clearly this batch cannot be accepted for the application.
- The diffraction peaks of brick 5 are much narrower than the peaks of the other bricks, i.e., the severely deformed ground surface layer of brick 5 was most probably removed by polishing. Therefore its good behavior in bending despite its relatively small compressive residual surface stresses is to be ascribed to its good surface finish combined with its acceptable structure (in terms of grain size and rolling deformation). Its residual stresses lower than that of other bricks are most probably due to the elimination of the highly stressed and deformed superficial layer.
- Brick 6 has a rough surface and its Young modulus is smaller than the modulus of the other samples (small but significant difference), despite its near theoretical density and absence of pores. Its relatively poor bending behavior in transverse direction should thus be related with its surface state, as its grain size seems to be the finest of the lot. There is no hint for the reason its Young modulus is smaller than expected.
- The density of brick 1 (measured by water displacement) was slightly smaller than the density of the bricks showing a better mechanical behavior (measured using the same technique). Remark however that the average value corresponds to only 2 measurements and its standard deviation is correspondingly very large: i.e., we do not consider significant its density difference with respect to the other “good” samples. Its Young modulus is the expected one for a fully dense tungsten. Reasons for the border-line behavior of its tensile strength are not yet clear.
- In conclusion, bricks 2, 4 and 5 are, in our opinion, acceptable from both mechanical behavior and structural point of view.